https://doi.org/10.1016/j.ejmech.2018.11.070

Design, Synthesis and Biological Evaluation of Quinoline-Indole Derivatives as Anti-tubulin Agents Targeting the Colchicine Binding Site

Wenlong Li[a], Wen Shuai[a], Honghao Sun[a], Feijie Xu[a], Yi Bi[b], Jinyi Xu[a,*], Cong Ma[c], Hequan Yao[a], Zheying Zhu[d], Shengtao Xu[a,*]

[a]State Key Laboratory of Natural Medicines and Department of Medicinal Chemistry, China Pharmaceutical University, 24 Tong Jia Xiang, Nanjing 210009, P. R. China

[b]School of Pharmacy, Key Laboratory of Molecular Pharmacology and Drug Evaluation, Yantai University, Yantai, 264005. P. R. China

[c]State Key Laboratory of Chemical Biology and Drug Discovery, and Department of Applied Biology and Chemical Technology, The Hong Kong Polytechnic University, Kowloon, Hong Kong

[d]Division of Molecular Therapeutics & Formulation, School of Pharmacy, The University of Nottingham, University Park Campus, Nottingham NG7 2RD, U. K.

***Corresponding Author:**
E-mail addresses: jinyixu@china.com (J. Xu); cpuxst@163.com (S. Xu).

Abstract

A series of novel isocombretastatin A-4 (isoCA-4) analogs were designed and synthesized by replacing 3,4,5-trimethoylphenyl and isovanillin of isoCA-4 with quinoline and indole moieties, respectively. The structure activity relationships (SARs) of these synthesized quinoline-indole derivatives have been intensively investigated. Two compounds **27c** and **34b** exhibited the most potent activities against five cancer cell lines with IC_{50} values ranging from 2 to 11 nM, which were comparable to those of Combretastatin A-4 (CA-4, **1**). Further mechanism investigations revealed that **34b** effectively inhibited the microtubule polymerization by binding to the colchicine site of tubulin. Further cellular mechanism studies elucidated that **34b** disrupted cell microtubule networks, arrested the cell cycle at G2/M phase, induced apoptosis and depolarized mitochondria of K562 cells. Moreover, **34b** displayed potent anti-vascular activity in both wound healing and tube formation assays. Importantly, **27c** and **34b** significantly inhibited tumor growth in H22 xenograft models without apparent toxicity, suggesting that **27c** and **34b** deserve further research as potent antitumor

agents for cancer therapy.

Key words: quinoline; indole; microtubule; tubulin inhibitor; colchicine binding site; antitumor

1. Introduction

CA-4 (**1**) (Figure 1) was a natural *cis*-stilbene derivative which was isolated from the bark of the African willow tree *Combretum caffrum* [1]. It has been identified as a typical tubulin polymerization inhibitor that target the colchicine binding site [2]. CA-4 displayed potent cytotoxicity against a wide range of cancer cell lines including multidrug resistant (MDR) cells at nanomolar levels [3]. Moreover, CA-4P, the phosphate prodrug of CA-4, induced vascular shutdown within tumors at doses less than one-tenth of the maximum tolerated dose, demonstrating the clinical potential of CA-4P as vascular disrupting agent [4]. CA-4P had been evaluated in clinical trials, however, it had been discontinued due to the lack of a meaningful improvement in progression-free survival (PFS) and unfavorable partial response data [5]. The *Z*-isomer of CA-4 is prone to isomerization to produce the *E*-isomer during storage, administration and metabolization, that is significantly less potent at inhibiting tubulin polymerization and cancer cell growth [6,7]. The isomerization could be avoided by the discoveries of Phenstatin (**3**) and isoCA-4 (**4**) [8,9]. IsoCA-4 held the similar properties as CA-4 but was more metabolically stable than CA-4 [10]. Other similar 1,1-diarylethylene derivatives such as compounds **5**-**9**, which have more restricted conformations than isoCA-4, were also discovered [11-14]. Another interesting isoCA-4 analog **10** was synthesized by replacing two hydrogens of the olefinic linker of isoCA-4 with two fluorine atoms, which was about 3-fold more potent than isoCA-4 against HCT-116 cells [15].

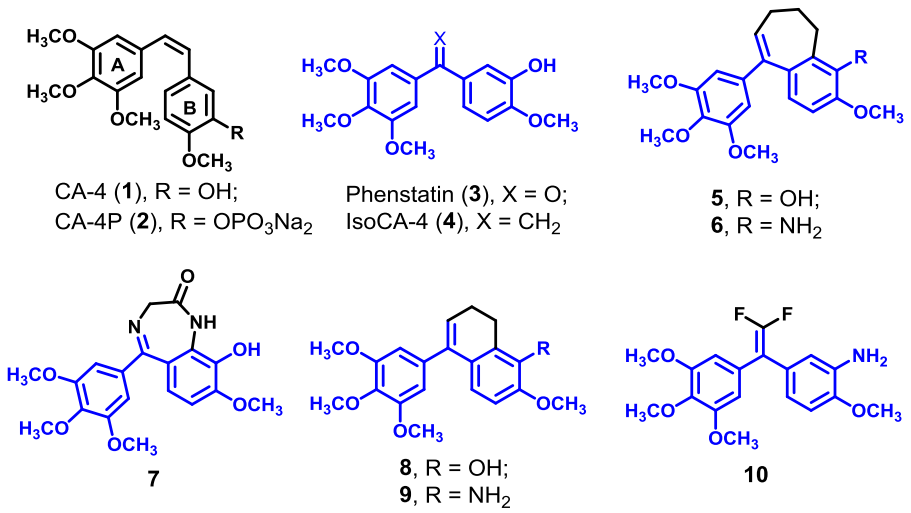

Fig. 1. CA-4, isoCA-4 and isoCA-4 analogs.

Nitrogenous heterocycles have been utilized in the construction of colchicine binding site inhibitors (CBSIs) [16, 17]. Quinazoline containing compounds such as **11**-**15** (Fig. 2) were discovered with potent anti-tubulin activities [18-22]. Recently, isoCA-4 analog **16** with a quinoline moiety was reported by Alami's group, and the docking studies of **16** showed that the *N*-1 atom of quinoline formed a hydrogen bond with the critical residue Cys 241 [23, 24], which demonstrated that quinoline moiety might be a surrogate of the traditional 3,4,5-trimethoylphenyl moiety when binding to the colchicine site. Meanwhile, indole moiety has also been found to occur in the structures of CBSIs, especially for the replacement of isovanillin ring [25-27]. CA-4 analog **17** and isoCA-4 analogs **18**, **19** containing indole moieties were discovered with both potent anti-tubulin and antitumor activities [28-30].

In recent years, our group has focused on discovering and developing novel anti-cancer agents targeting tubulin-microtubule system, such as chalcone analogs bearing vinyl sulfone skeleton [31], 4-arylisochromenes [32], and quinazolines that occupy three zones of colchicine domain [33]. In this work, we further designed a series of novel quinoline-indole derivatives by replacing 3,4,5-trimethoylphenyl and isovanillin moieties of isoCA-4 with quinoline and indole rings, respectively (Fig. 2). Herein, we report the synthesis and evaluation of their anticancer activities *in vitro* and *in vivo*. In addition, the underlying cytotoxic mechanisms of the representative compound **34b** are also elucidated.

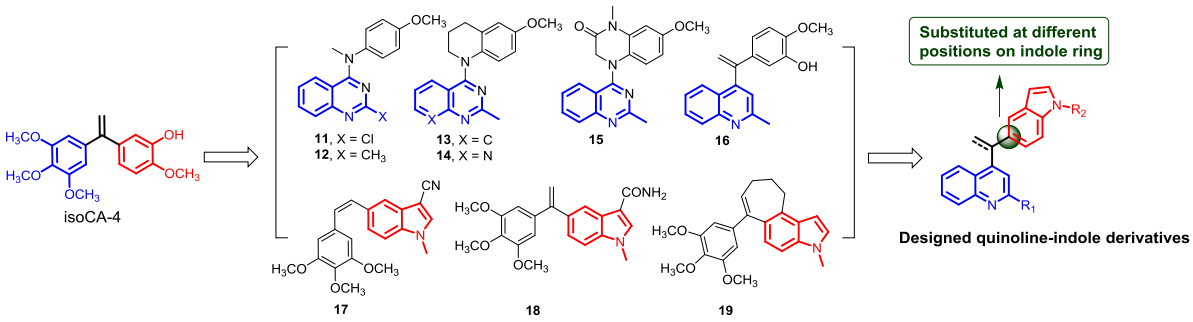

Fig. 2. Design strategy of quinoline-indole derivatives as isoCA-4 analogs.

2. Results and discussion

2.1 Chemistry

Quinoline-indole derivatives **26a-d** with different substituted positions on the indole ring were synthesized by the method in Alami's report [23] as shown in Scheme 1. Acetylindoles **21a-c** were prepared by three different methods. 3-Acetyl-6-methoylindole (**21a**) was synthesized by a Vilsmeier-Haack reaction of 6-methoylindole (**20**) in the presence of phosphoryl chloride and dimethylacetamide.

Nucleophilic attack on the aldehyde of indole-4-aldehyde (**22**) by methylmagnesium bromide (CH_3MgBr) followed by oxidization produced 4-acetylindole (**21b**). 5-Acetylindole (**24**) was prepared by the reaction of indole-5-acid (**23**) with lithium methide (CH_3Li), the *N*-1 of which was then protected to afford *N*-Boc-5-acetylindole (**21c**). Subsequently, acetylindoles **21a-c** were transformed into their corresponding *N*-tosylhydrazones **25a-c** which were then coupled with 4-chlorine-2-methylquinoline via Pd-catalyzed cross coupling reactions to afford target compounds **26a-c** in moderate to good yields, and **26c** was deprotected to produce **26d**.

Scheme 1. The synthetic route for target compounds **26a-d**[a].

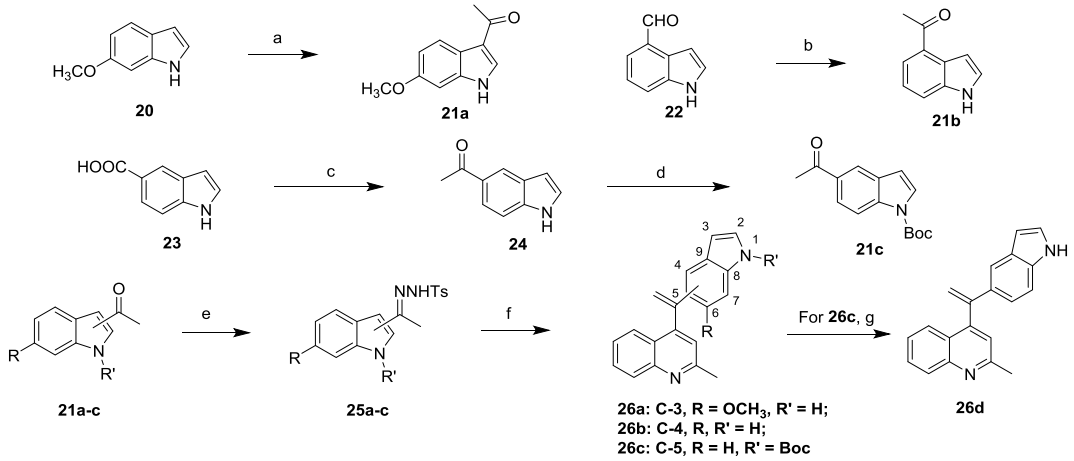

[a]Reagents and conditions: (a) $POCl_3$, DMA, 0 ℃ to rt, 2 h, 89.6%; (b) i) CH_3MgBr, THF, 0 ℃ to rt, 1 h; ii) IBX, DMSO; 35.2% over two steps; (c) CH_3Li, THF, rt, 1 h, 72.9%; (d) NaH, $(Boc)_2O$, THF, rt, 1 h, 79.9%; (e) *p*-Toluenesulfonhydrazide, EtOH, 90 ℃, 2 h; (f) 4-Chlorine-2-methylquinoline, $PdCl_2(CH_3CN)_2$, Xphos, *t*-BuOLi, 90 ℃, 2 h, 50.2-70.5%; (g) K_2CO_3, CH_3OH, reflux, 2 h, 90.9%.

Scheme 2. The synthetic route for target compounds **27a-d**, **28a-c**, **30a-c** and **33a-c**[a].

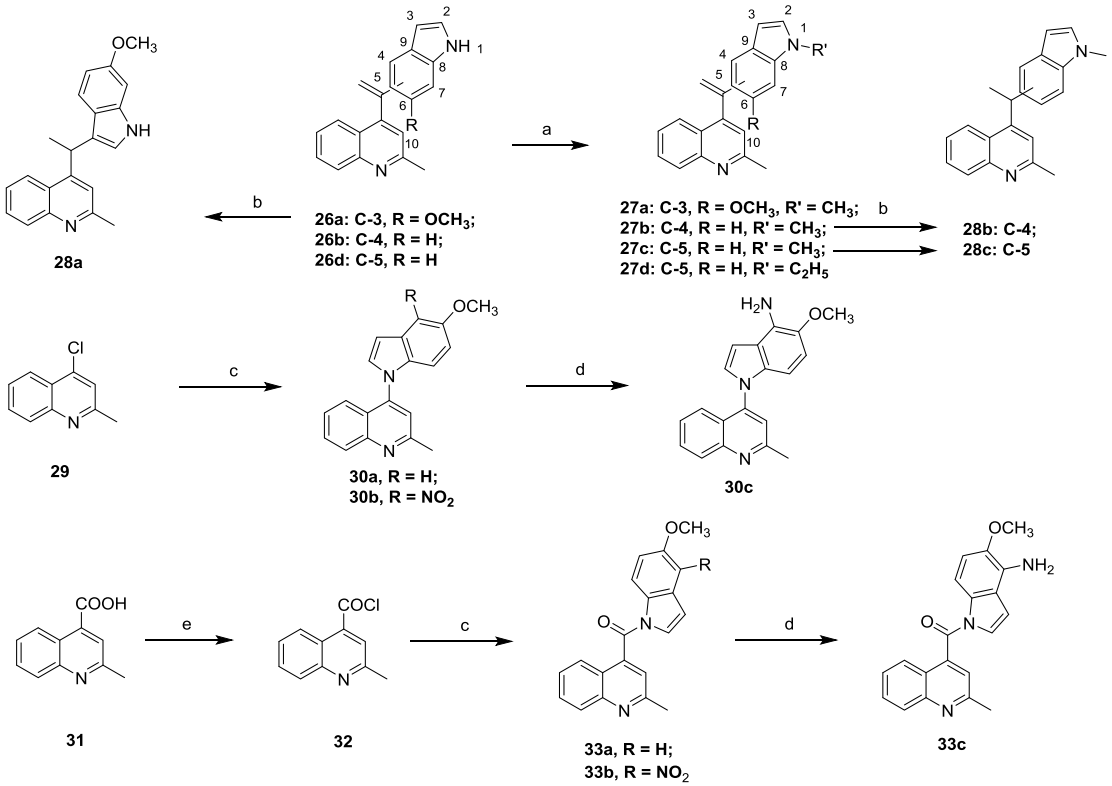

Reagents and conditions: (a) NaH, CH_3I or C_2H_5I, THF, 0 ℃ to rt, 30 min, 72.0-85.2%; (b) Pd/C, H_2, CH_3OH, overnight, rt, 60.0-72.3%; (c) NaH, 5-methoylindole or 4-nitro-5-methoylindole, DMF, 50 ℃, 25.5-39.4%; (d) Fe, AcOH, EtOH, reflux; 68.0-72.2%; (e) Oxalyl chloride, DMF (cat.), DCM, 0 ℃ to rt, 30 min.

Methyl or ethyl groups were introduced to *N*-1 position of **26a**, **26b** and **26d** to afford target compounds **27a-d (**Scheme 2**)**. **26a**, **27b**, and **27c** were then reduced in the presence of Pd/C under H_2 atmosphere to give target compounds **28a-c** as racemic mixtures. Compounds **30a-c** and **33a-c**, of which quinoline moieties were substituted at *N*-1 position of indole, were also synthesized using 4-chlorine-2-methylquinoline (**29**) and 2-methylquinoline-4-acid (**31**) as the starting materials, respectively. Compounds **34a-c** with different substitutions at *N*-1 position of indole were also synthesized as depicted in Scheme 3.

Target compounds **35a-i** that have different substitutions at C-2 position of quinoline were synthesized as outlined in Scheme 4. Aldehyde **35a** was produced by the oxidation of **27c** in the presence of selenium dioxide (SeO_2), followed by reduction with sodium borohydride ($NaBH_4$) to give compound **35b**. Target compounds **35c-i** were prepared by the cross-coupling reactions with various C-2 substituted quinolines **36c-i** and *N*-tosylhydrazone **37**.

Scheme 3. The synthetic route for target compounds **34a-c**[a].

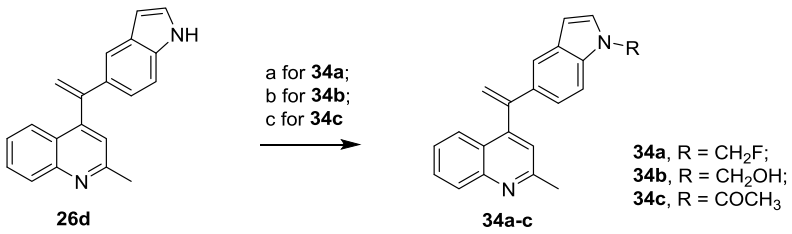

[a]Reagents and conditions: (a) NaH, $ClCH_2F$, DMF, sealed tube, 80 ℃, 2 h, 18.0%; (b) 10% NaOH aqueous, HCHO aqueous, EtOH, rt, 2 h, 64.9%; (c) Ac_2O, Et_3N, DCM, reflux, overnight, 78.9%.

Scheme 4. The synthetic route for target compounds **35a-i**[a].

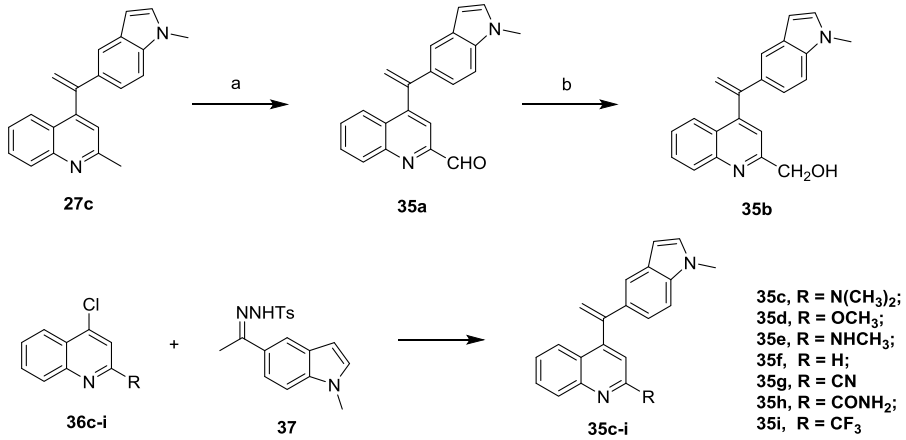

[a]Reagents and conditions: (a) SeO_2, EtOH, 80 ℃, 2 h, 38.5%; (b) $NaBH_4$, THF, rt, 30 min, 75.0%; (c) $PdCl_2(CH_3CN)_2$, Xphos, *t*-BuOLi, 90 ℃, 2 h, 40.7-80.0%.

2.2 In vitro antiproliferative studies

To identify the best substituted position on the indole ring, fourteen compounds **26a-d**, **27a-c**, **28a-c**, **30a**, **30c**, **33a** and **33c** were evaluated first for their antiproliferative activities against K562 cells. As shown in Table 1, compounds **26a**, **26b**, **27b**, **28a** and **28b**, of which olefin was substituted at C-3 and C-5 position on the indole rings, displayed lower activities (IC_{50} > 1 μM) than the C-4 substituted counterparts **26d**, **27c** and **28c**. Besides, the methyl substituted at *N*-1 position of indole (**27c**) significantly increased the activity for about 60 folds when compared to the non-substituted counterpart **26d**. The reduction of the olefin declined the activity as compared by **27c** and **28c**. Compounds **30a**, **30c**, **33a** and **33c**, of which quinoline moieties were linked to *N*-1 position of indole rings, were also designed and evaluated for their activities, and the results showed that compounds **30c** and **33c** with amino groups substituted at C-4 position of indole rings exhibited decent activities. Furthermore, the effects of substitutions at *N*-1 position of indole ring on activity were investigated, compounds containing methyl (**27c**, IC_{50} = 2 nM) and hydroxymethyl (**34b**, IC_{50} = 2 nM) groups were more potent than other groups including ethyl (**27d**,

IC_{50} = 31 nM), fluoride methyl (**34a**, IC_{50} = 153 nM), or acetyl (**34c**, IC_{50} = 179 nM). Moreover, the effects of substitutions at C-2 position of quinoline moiety on activity were studied, compounds **35a** (CHO), **35b** (CH_2OH), **35c** (dimethylamino), **35d** (OCH_3), **35e** ($NHCH_3$), **35f** (H), **35g** (CN), **35h** ($CONH_2$) and **35i** (CF_3) all exhibited less potent activities than **27c** (CH_3).

Five cancer cell lines including human hepatocellular carcinoma (HepG2), epidermoid carcinoma of the nasopharynx (KB), human colon cancer cells (HCT-8) human breast cancer cells (MDA-MB-231), mouse liver cancer cells (H22), and human normal hepatocytes LO2 cells were chosen to further evaluate the antiproliferative activities of representative compounds. The cytotoxic data in Table 2 showed that all these selected compounds displayed potent activities against these five cancer cell lines in nanomolar ranges, and they also exhibited good selectivities against LO2 cells. The K562 cell was the most sensitive cell line among six cancer cell lines tested. Compounds **27c** and **34b** that showed the most potent activities against K562 cells also displayed very potent activities against these five cancer cell lines with IC_{50} values ranging from 5 to 11 nM, which were comparable to those of CA-4. The overall SARs of synthesized compounds were summarized in Fig. 3.

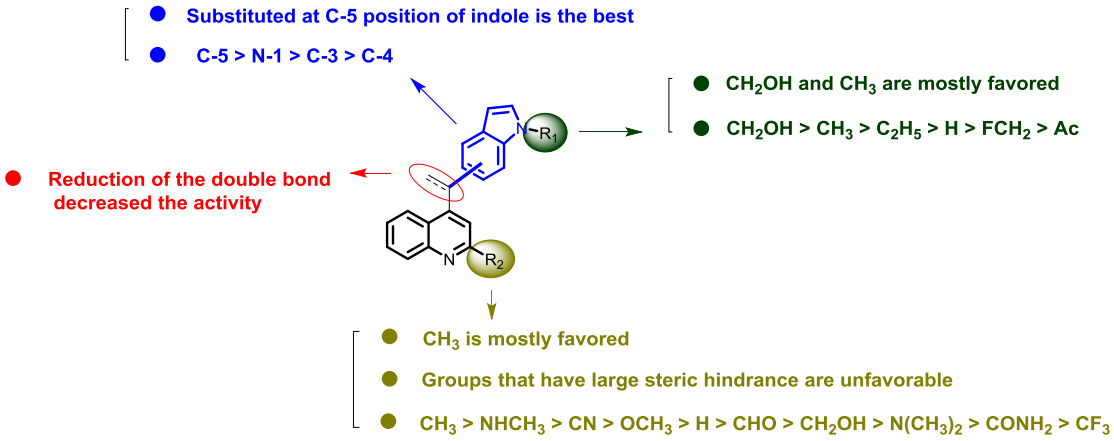

Fig. 3. Summarized SARs of target compounds.

To investigate whether our compounds are efficacious against drug resistant cancer cells, **27c** and **34b** were tested for their antiproliferative efficacy in the drug-resistant and parental sensitive cells using the MTT assay. As shown in Table 3, except for the adriamycin-resistant cell line Bel-7402/ADR, the drug-resistant indexes of **27c** and **34b** were comparable to those of CA-4, while positive drugs paclitaxel and vincristine exhibited 92.5-241.0 folds resistances to the corresponding drug-resistant cells. These results indicated that **27c** and **34b** also exhibited moderate antiproliferative efficacy against drug resistant cancer cells.

Table 1. The antiproliferative activities of all target compounds against K562 cells[a].

Compd.		IC_{50} K562 (μM)[b]	Compd.		IC_{50} K562 (μM)[b]
26a	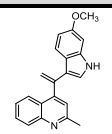	> 1	**33c**	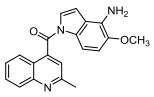	0.289 ± 0.032
26b	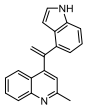	> 1	**34a**	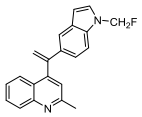	0.153 ± 0.015
26c	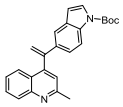	> 1	**34b**	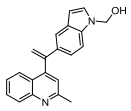	0.002 ± 0.001
26d	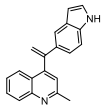	0.121 ± 0.012	**34c**	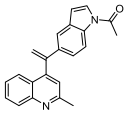	0.179 ± 0.010
27a	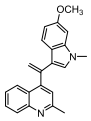	0.106 ± 0.009	**35a**	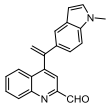	0.094 ± 0.006
27b	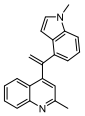	> 1	**35b**	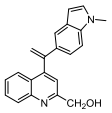	0.123 ± 0.011
27c	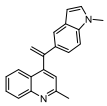	0.002 ± 0.001	**35c**	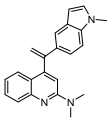	0.171 ± 0.018
27d	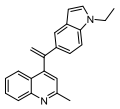	0.031 ± 0.005	**35d**	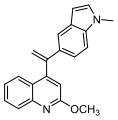	0.046 ± 0.009
28a	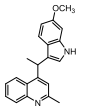	> 1	**35e**	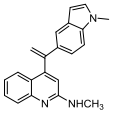	0.005 ± 0.001
28b	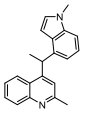	> 1	**35f**	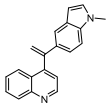	0.090 ± 0.007
28c	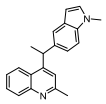	0.037 ± 0.009	**35g**	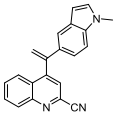	0.008 ± 0.001
30a	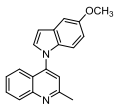	> 1	**35h**	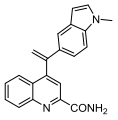	0.282 ± 0.025
30c	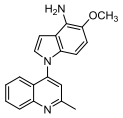	0.079 ± 0.005	**35i**	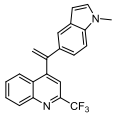	0.446 ± 0.035
3a	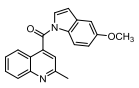	> 1	**CA-4**	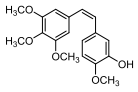	0.007 ± 0.001

[a] Cells were treated with different concentrations of the compounds for 72 h. Cell viability was measured by the

MTT assay as described in the Experimental Section.

[b] IC_{50} values are indicated as the mean ± SD (standard error) of at least three independent experiments.

Table 2. Antiproliferative activities of representative compounds against five cancer cell lines and normal human liver cells[a].

Compd.	IC_{50} values (μM)[b]					
	HepG2	KB	HCT-8	MDA-MB-231	H22	LO2
26d	0.377 ± 0.022	0.372 ± 0.035	0.403 ± 0.040	0.204 ± 0.021	0.184 ± 0.020	0.881 ± 0.105
27c	0.011 ± 0.002	0.008 ± 0.001	0.009 ± 0.001	0.009 ± 0.002	0.008 ± 0.001	0.088 ± 0.021
28c	0.101 ± 0.018	0.109 ± 0.013	0.096 ± 0.009	0.103 ± 0.009	0.120 ± 0.012	0.214 ± 0.015
34b	0.006± 0.001	0.005 ± 0.001	0.007 ± 0.001	0.006 ± 0.001	0.006 ± 0.001	0.048 ± 0.010
35d	0.053± 0.011	0.084 ± 0.014	0.103 ± 0.015	0.112 ± 0.015	0.105 ± 0.010	0.197 ± 0.032
35e	0.020± 0.004	0.008 ± 0.002	0.010 ± 0.001	0.027 ± 0.005	0.025 ± 0.003	0.085 ± 0.020
35g	0.011± 0.002	0.022 ± 0.003	0.028 ± 0.004	0.034 ± 0.005	0.022 ± 0.004	0.055 ± 0.011
CA-4	0.009± 0.002	0.011 ± 0.002	0.011 ± 0.002	0.011 ± 0.003	0.010 ± 0.002	0.046 ± 0.010

[a] Cells were treated with different concentrations of the compounds for 72 h. Cell viability was measured by the MTT assay as described in the Experimental Section.

[b] IC_{50} values are indicated as the mean ± SD (standard error) of at least three independent experiments.

Table 3. The IC_{50} values of representative compounds in different drug-resistant cancer cells.

Compd.	IC_{50} values (μM)[a]											
	HCT-8	HCT-8/Taxol	DRI[b]	A549	A549/Taxol	DRI	K562	K562/VCR	DRI	Bel-7402	Bel-7402/ADR	DRI
27c	0.009 ± 0.001	0.098 ± 0.018	10.9	0.025± 0.002	0.342 ± 0.032	13.7	0.002 ± 0.001	0.030 ± 0.003	15	0.028 ± 0.003	0.185 ± 0.022	6.6
34b	0.007 ± 0.002	0.088 ± 0.022	12.6	0.009 ± 0.002	0.119 ± 0.022	13.2	0.002 ± 0.001	0.031 ± 0.005	15.5	0.010 ± 0.002	0.061 ± 0.009	6.1
CA-4	0.011 ± 0.002	0.087 ± 0.005	7.9	0.009 ± 0.002	0.175 ± 0.022	19.4	0.007 ± 0.001	0.057± 0.012	8.1	0.011 ± 0.002	0.058 ± 0.002	5.3
ADR	ND[c]	ND	-	ND	ND	-	ND	ND	-	0.274 ± 0.086	1.732 ± 0.202	6.3
Taxol	0.028 ± 0.004	2.590 ± 0.122	92.5	0.018 ± 0.004	1.830 ± 0.104	101.6	ND	ND	-	ND	ND	-
VCR	ND	ND	-	ND	ND	-	0.021± 0.004	5.060 ± 0.562	241.0	ND	ND	-

[a] Data are presented as the mean ± SD from the dose-response cures of at least three independent experiments.

[b] DRI: drug-resistant index = (IC_{50} of drug resistant cancer cell) / (IC_{50} of parental cancer cell).

[c] ND: not detected.

2.3 In vitro tubulin polymerization inhibitory assay

To elucidate whether these quinoline-indole derivatives target the tubulin-microtubule system, two most potent compounds **27c** and **34b** were evaluated for their effects on microtubule dynamics of K562 cells. The typical microtubule-destabilizing agent (MDA) colchicine and microtubule-stabilizing agent taxol were employed as the controls. As shown in Fig. 4, taxol exhibited a significant promotion of tubulin polymerization, while colchicine produced a significant inhibition of tubulin polymerization. Compounds **27c** and **34b** displayed similar actions to that of colchicine, indicating that **27c** and **34b** were MDAs. The calculated IC_{50} values of **27c** and **34b** in inhibiting tubulin polymerization were 2.54 and 2.09 μM, respectively, which were comparable to that of CA-4 (IC_{50} = 2.12 μM) (Table 4). In addition, **27c** and **34b** competed with [3H]-colchicine in binding to tubulin. The binding potency of **27c** and **34b** to the colchicine binding site was 89.4% and 90.5% at 5 μM, respectively (Table 4), indicating that **27c** and **34b** bind to the colchicine binding site. Therefore, taking considerations of the good activities of compound **34b** showing both in the *in vitro* antiproliferative assay and tubulin polymerization inhibition assay, it was selected for further mechanism studies.

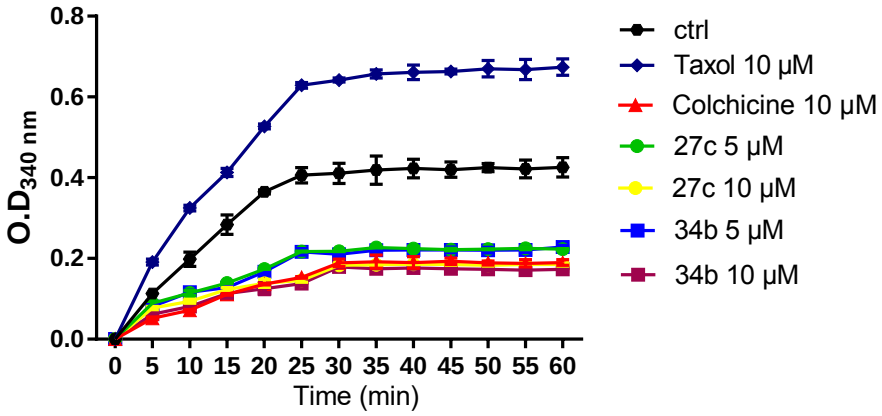

Fig. 4. Effects of **27c** and **34b** on tubulin polymerization *in vitro*. Purified tubulin protein at 2 mg/mL in a reaction buffer was incubated at 37 °C in the presence of 1% DMSO, test compounds (**27c** at 5 or 10 μM), (**34b** at 5 or 10 μM), Colchicine (10 μM) or Taxol (10 μM). Polymerizations were followed by an increase in fluorescence emission at 350 nm over a 60 min period at 37 °C. The experiments were performed three times.

Table 4. Inhibition of tubulin polymerization[a] and colchicine binding to tubulin[b]

Compd.	Inhibition of tubulin polymerizaion	Inhibition of colchicine binding (%) inhibition ± SD	
	IC_{50} (μM)	1 μM	5 μM

27c	2.54 ± 0.13	78.4 ± 1.9	89.4 ± 2.2
34b	2.09 ± 0.20	79.4 ± 2.2	90.5 ± 2.5
CA-4	2.12 ± 0.10	80.2 ± 2.1	91.5 ± 4.0

[a] The tubulin assembly assay measured the extent of assembly of 2 mg/mL tubulin after 60 min at 37 °C. Data are presented as mean from three independent experiments.

[b] Tubulin, 1 μM; [3H]-colchicine, 5 μM; and inhibitors, 1 or 5 μM.

2.4. Anti-microtubule effects in K562 cells

To study whether **34b** could disrupt the microtubule dynamics in living cells, immunofluorescent assay in K562 cells were performed. As shown in Fig. 5, K562 cells in the control group exhibited normal arrangement and organization. However, after treatments with **34b** (1 nM, 2 nM, and 4 nM) for 24 h, the microtubule networks in cytosol were disrupted; these results indicated that **34b** can induce a dose-dependent collapse of the microtubule networks.

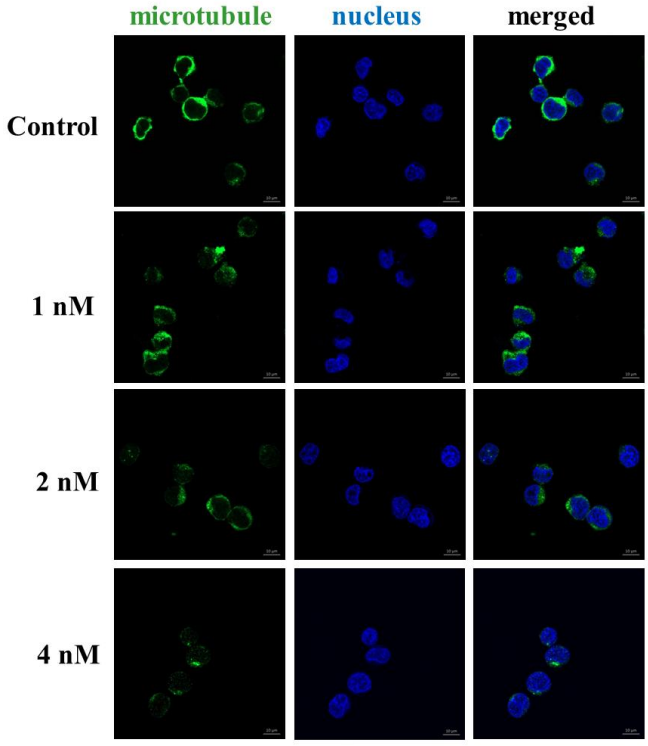

Fig. 5. Effects of **34b** on the cellular microtubule networks visualized by immunofluorescence. K562 cells were treated with vehicle control 0.1% DMSO, **34b** (1 nM), **34b** (2 nM), and **34b** (4 nM). Then, the cells were fixed and stained with anti-α-tubulin−FITC antibody (green), Alexa Fluor 488 dye and counterstained with DAPI (blue). The detection of the fixed and stained cells was performed with an LSM 570 laser confocal microscope (Carl Zeiss, Germany).

2.5 Cell cycle analysis

As most tubulin destabilizing agents could disrupt the cell cycle distribution, a flow cytometry analysis was performed to examine the effect of **34b** on K562 cell cycle progression using a propidium iodide (PI) staining assay. As illustrated in Fig. 6a and 6b, incubation with **34b** blocked the cell cycle at the G2/M phase. Compared to the control cells incubated with DMSO, the incubation of K562 cells with increased concentrations of **34b** (1, 2, and 4 nM) increased the percentage of cells at the G2/M phase from 10.51% to 23.21%.

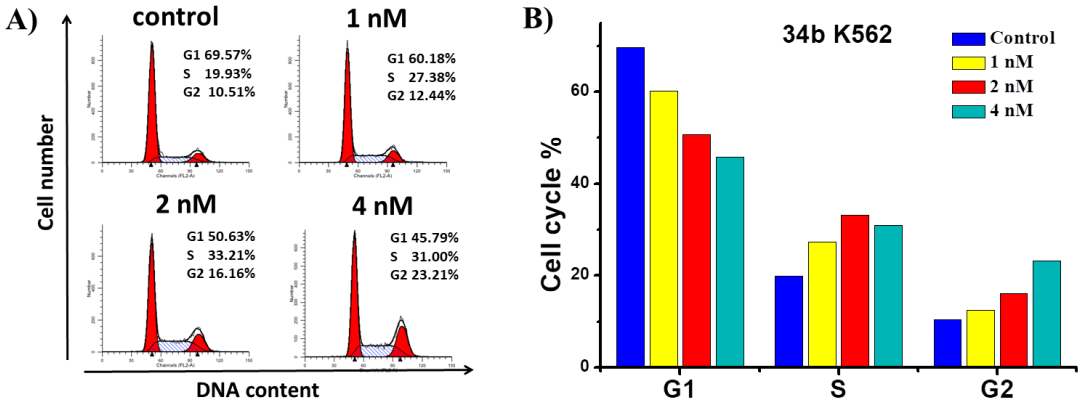

Fig. 6. (A) Compound **34b** induced G2/M arrest in K562 cells. K562 cells were incubated with varying concentrations of **34b** (0, 1, 2, and 4 nM) for 48 h. Cells were harvested and stained with PI and then analyzed by flow cytometry. The percentages of cells in different phases of cell cycle were analyzed by ModFit 4.1. (B) Histograms display the percentage of cell cycle distribution after treatment with **34b**.

2.6 Cell apoptosis analysis

To assess whether compound **34b** would induce cell apoptosis, an Annexin V-FITC/ PI assay was carried out. As shown in Fig. 7A and 7B, compound **34b** induced K562 cell apoptosis in a dose-dependent manner. The percentage of apoptotic cells after 48 h treatment was only 5.96% in the control group. When the cells were incubated with **34b** at 1, 2, and 4 nM for 48 h, the total numbers of early (Annexin-V+/PI−) and late (Annexin-V+/PI+) apoptotic cells were 25.7%, 54.9% and 72.8%, respectively. These results demonstrated that compound **34b** effectively induced cell apoptosis of K562 cells in a dose-dependent manner.

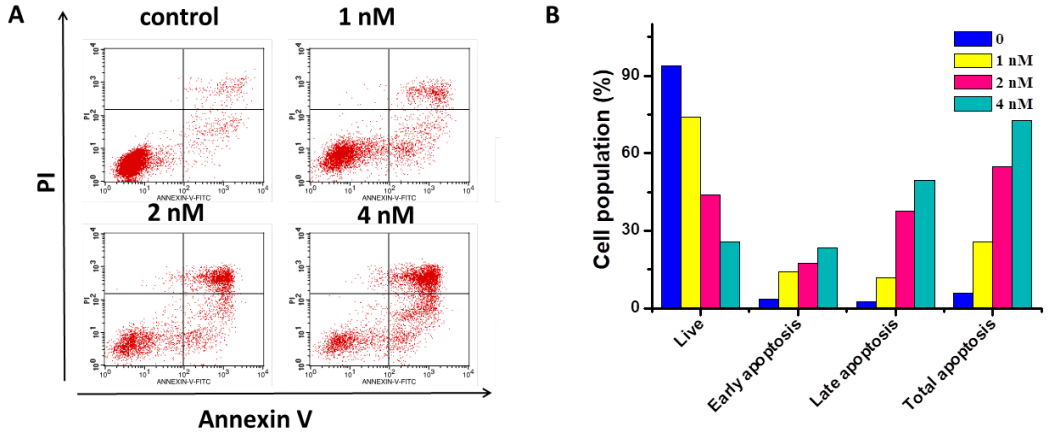

Fig. 7. (A) Compound **34b** induced apoptosis in K562 cells. K562 cells were incubated with varying concentrations of **34b** (0, 1, 2, and 4 nM). After 48 h of incubation, cells were collected and stained with Annexin V/PI, followed by flow cytometric analysis. The percentages of cells in each stage of cell apoptosis were quantified by flow cytometry: (upper left quadrant) necrosis cells; (upper right quadrant) late-apoptotic cells; (bottom left quadrant) live cells; and (bottom right quadrant) early apoptotic cells. (B) Histograms display the percentage of cell distribution after treatment with **34b**.

2.7 Mitochondrial membrane potential analysis.

In order to determine whether **34b**-induced apoptosis was involved in a disruption of mitochondrial membrane integrity, the fluorescent probe JC-1 was employed to measure the mitochondrial membrane potential (MMP). When treated with **34b** at concentrations of 0, 1, 2 and 4 nM for 48 h, the number of K562 cells with collapsed MMP increased from 6.17% to 28.99%, 45.10% and 73.55%, respectively. (Fig. 8), suggesting that **34b** caused mitochondrial depolarization of K562 cells in the process of apoptosis.

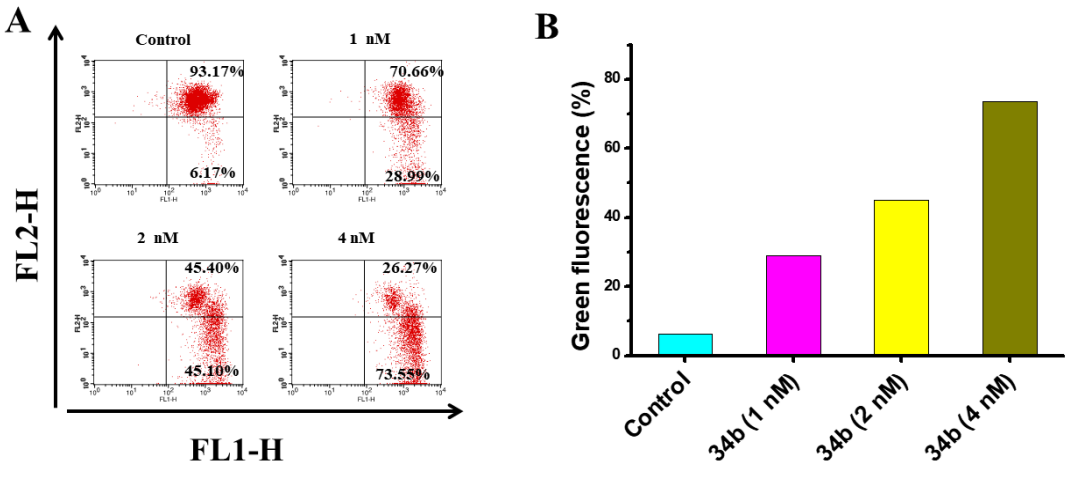

Fig. 8. Effects of **34b** on the mitochondrial membrane potential of K562 cells. (A) Incubation with different concentrations (0, 1, 2, and 4 nM) of **34b** in K562 cells for 48 h prior to staining with JC-1 dye, the number of cells with collapsed mitochondrial membrane potentials was determined by flow cytometry analysis. (B) Histograms display the percentage of green fluorescence.

2.8 In vitro evaluation of anti-vascular activity

To evaluate the anti-vascular activity of compound **34b**, the human umbilical vein endothelial cells (HUVECs) culture assays were firstly performed to assess the ability of **34b** to inhibit HUVECs migration which is the key step to generate new blood vessels. As shown in Fig. 9A, the untreated cells migrated to fill the area that was initially scraped after 24 h. In contrast, **34b** significantly inhibited the HUVEC migration in a dose-dependent manner (Fig. 9C).

The HUVEC tube formation is the key step in angiogenesis, including proliferation, adhesion, and the formation of tube-like vascular structures. Then, we evaluated the anti-vascular activity of **34b** in a tube formation assay. After being seeded on Matrigel, HUVECs form the capillary-like tubules with multicentric junctions (Fig. 9B, the control group), while **34b** inhibited HUVEC cord formation in a concentration-dependent manner at concentrations (1, 2 and 4 nM) that had minimal effects on HUVEC proliferation after treated with **34b** for 6 h. These results showed that compound **34b** effectively inhibited the tube formation of HUVECs.

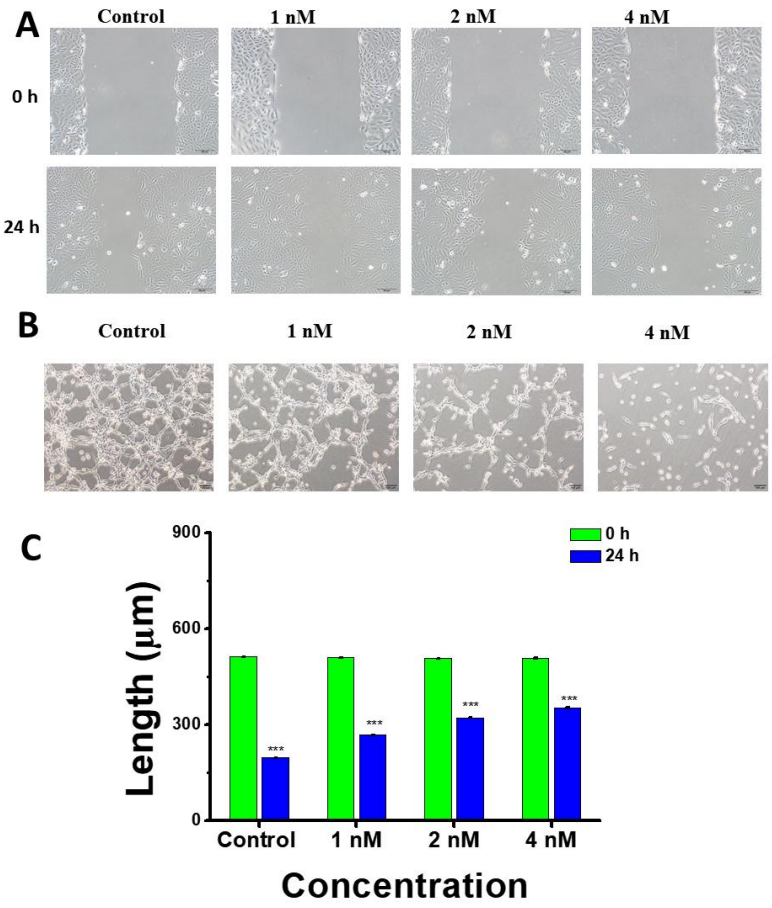

Fig. 9. Effects on the HUVECs migration and tube formation. (A) Scratches were created with sterile 200 μL pipette and images were captured using phase contrast microscopy at 0 h and 24 h after treatments with 0, 1, 2 and 4 nM of **34b**. (B) Images depicting the formation of HUVEC capillary-like tubular network by treatments with 0, 1, 2 and 4 nM of **34b** for 6 h. (C) Histograms display the length of the scratches at 0 h and 24 h after treatments with 0, 1, 2 and 4 nM of **34b**, *** $P < 0.001$, vs control group.

*2.9 In vivo antitumor activity of **27c** and **34b***

To evaluate the *in vivo* antitumor activities of **27c** and **34b**, liver cancer xenograft mouse model was established by subcutaneous inoculation of H22 cells into the right flank of mice. The tumor size and body weights of the mice were monitored and recorded every 2 days. Paclitaxel (PTX), CA-4 and the disodium phosphate of CA-4 (CA-4P) were selected as the positive controls. As shown in Fig. 10A and Fig. 10B, **27c** and **34b** at the dose of 20 mg/kg per day significantly decreased the tumor volume. The reduction in tumor weight reached 72.7% at a dose of 6 mg/kg per 2 days (i.v.) of PTX at 21 days after initiation of treatment as compared to vehicle, while **27c** and **34b** reduced tumor weights by 63.7% and 57.3% at doses of 20 mg/kg per day (i.v.), respectively. Notably, **27c** at the dose of 20 mg/kg displayed more

potent antitumor activity than CA-4 (inhibition rate: 51.0% at 20 mg/kg) or CA-4P (inhibition rate: 62.7% at 20 mg/kg) (Fig. 10D). Moreover, **27c** and **34b** did not significantly affected body weight even at the doses of 20 mg/kg, while treatment with PTX at a dose of 6 mg/kg per 2 days had significant effects on body weight (Fig. 10C). Thus, compounds **27c** and **34b** are worthy of further investigations for the treatment of cancers.

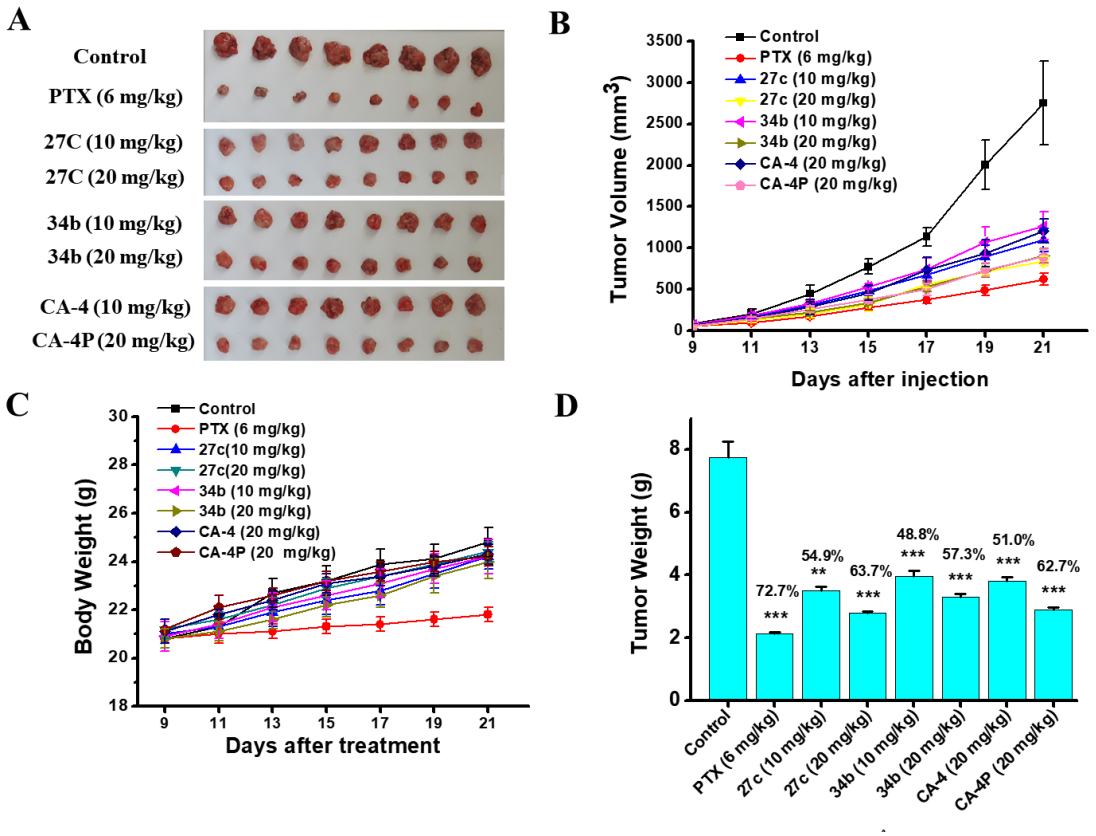

Fig. 10. **27c** and **34b** inhibited liver cancer xenograft growth *in vivo*. After administered with vehicle, PTX (6 mg/kg per 2 days), **27c** (10 mg/kg per day), **27c** (20 mg/kg per day), **34b** (10 mg/kg per day), **34b** (20 mg/kg per day), CA-4 (20 mg/kg per day), and CA-4P (20 mg/kg per day) for three weeks, the mice were sacrificed, and the tumors were weighted. (a) The images of tumors from mice at 21 days after initiation of treatment. (b) Tumor volume changes of mice during treatment. (c) Body weight changes of mice during treatment. (d) The weight of the excised tumors of each group. $^{**}P < 0.05$, $^{***}P < 0.001$, vs control group.

2.10 Molecular modelling studies

To illustrate the binding modes of two most active compounds **27c** and **34b** with tubulin, we performed a docking study of **27c** and **34b** into the colchicine binding pocket of tubulin (PDB: 5lyj) by using the DOCK program in the Discovery Studio 3.0 software. As shown in Fig. 11A and Fig. 11B, **27c** or **34b** and CA-4 adopted very similar positioning at the colchicine binding pocket. The *N*-1 of quinoline moiety formed hydrogen bonds with residue Cys241, which were similar to that of the

4-methoyl group of CA-4. The indole rings extended into the hydrophobic pocket which was surrounded by residues Thr179, Val315, Asn350 and Val351. The hydroxymethyl group of **34b** formed two additional hydrogen bonds with Val315 and Asn350, which might explain the slight difference in activity between **27c** and **34b**. The binding modes of **27c** and **34b** resembled to that of compound **16** predicted by Alami's group [23], which further demonstrated that quinoline moiety is a surrogate of the traditional 3,4,5-trimethoylphenyl moiety when binding to the colchicine site.

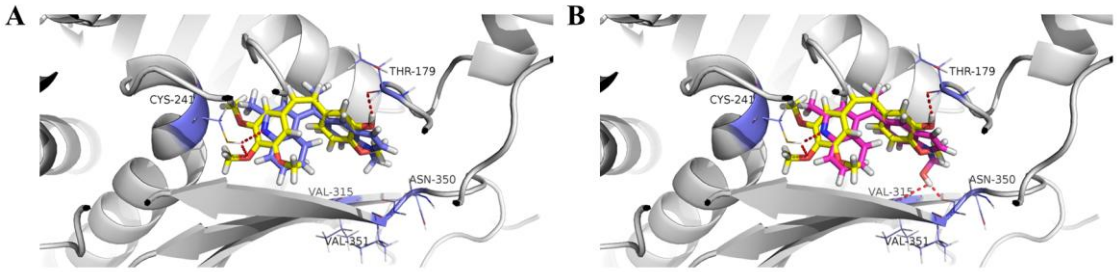

Fig. 11. (A) Proposed binding model for **27c** (violet) binding with tubulin (PDB code: 5lyj), and overlapping with CA-4 (yellow); (B) Proposed binding model for **34b** (magenta) binding with tubulin (PDB code: 5lyj), and overlapping with CA-4 (yellow).

3. Conclusion

In summary, we have designed, synthesized, and evaluated a series of novel quinoline-indole derivatives as tubulin polymerization inhibitors for cancer therapy. The SARs of these synthesized quinoline-indole derivatives have been intensively investigated. Two compounds **27c** and **34b** exhibited the most potent activities against five cancer cell lines with IC_{50} values ranging from 2 to 11 nM, which were comparable to those of CA-4. **27c** and **34b** also displayed moderate selectivity for human normal hepatocytes LO2 cells, which might indicate their low toxicities. Besides, **27c** and **34b** exhibited moderate antiproliferative efficacy against several drug resistant cancer cells, which were comparable to those of CA-4. Furthermore, **27c** and **34b** effectively inhibited tubulin polymerization as MDAs with IC_{50} values of 2.54 and 2.09 μM, respectively. Colchicine competition inhibition assay and molecular modelling studies indicated that **27c** and **34b** bind to the colchicine binding site. Further mechanism studies demonstrated that **34b** disrupted microtubule networks, arrested cell cycle at G2/M phase, induced apoptosis and depolarized mitochondria of K562 cells with a dose-dependent manner. Furthermore, the wound healing and tube formation assays also identified **34b** as a novel vascular disrupting agent. Finally, the *in vivo* antitumor activity of **27c** and **34b** were validated in H22 liver cancer xenograft mouse model. **27c** effectively suppressed the tumor volume and reduced tumor weight by 63.7% at the dose of 20 mg/kg per day (i.v.) without

apparent toxicity, which was more potent than CA-4 and CA-4P. Collectively, these results highlighted the **27c** and **34d** as novel anti-tubulin agents with clinical potential for the treatment of cancers, which deserve to be further investigated.

4. Experimental

4.1. Chemistry

4.1.1. General

Most chemicals and solvents were purchased from commercial sources. Further purification and drying by standard methods were employed when necessary. ^{1}H NMR and ^{13}C NMR spectra were recorded on Bruker-300 spectrometers in the indicated solvents (TMS as internal standard). Data are reported as follows: chemical shift in ppm (d), multiplicity (s =singlet, d =doublet, t =triplet, q =quartet, brs = broad singlet, m = multiple), coupling constant (Hz), and integration. High Resolution Mass measurement was performed on Agilent QTOF 6520 mass spectrometer with electron spray ionization (ESI) as the ion source. Flash column chromatography was carried out using commercially available silica gel (200-300 mesh) under pressure.

*4.1.2 Synthesis of intermediate **21a**.*

To a solution of 6-methoylindole (300 mg, 2.04 mmol) in 5 mL DMA, $POCl_3$ (1.9 mL, 20.4 mmol) was added at 0 ℃. After stirring for 2 h at room temperature, the mixture was basified with 10% NaOH aqueous. The precipitates were collected by filtration, washed with water and dried to afford intermediate **21a** (346 mg, 89.6%) as yellow solid, the crude product was used without further purification. The spectral data of **21a** was in accordance with literature report [34].

*4.1.3 Synthesis of intermediate **21b**.*

To a solution of indole-4-aldehyde (500 mg, 3.45 mmol) in 20 mL anhydrous THF, a solution of CH_3MgBr in diethyl ether (3 M, 2.87 mL, 8.6 mmol) was added dropwise at 0 ℃ under N_2 atmosphere. After stirring for 1 h, the reaction was quenched by NH_4Cl aqueous, and extracted with CH_2Cl_2 (3 × 50 mL). The combined organic layers were then washed with brine, dried over anhydrous Na_2SO_4, and concentrated in vacuo to provide 240 mg 1-(1H-indol-4-yl)ethan-1-ol as colorless oil, which was dissolved into 10 mL DMSO, and IBX（500 mg, 1.79 mmol）was added in one potion. After stirring for 1 h, the mixture was diluted with 50 mL EtOAc, then washed with water (20 mL × 3), saturated brine, dried over anhydrous Na_2SO_4, and concentrated in vacuo to afford crude product, which was purified by column chromatography with petroleum/ethyl acetate (2:1) to give intermediate **21b** (193 mg, 35.2% over two steps). The spectral data of **21b** was inaccordance with literature

report [35].

*4.1.4 Synthesis of intermediate **21c**.*

To a solution of indole-5-acid (2.5 g, 15.5 mmol) in 30 mL anhydrous THF, a solution of CH_3Li (1.6 M, 30 mL, 51.2 mmol) in diethyl ether was added dropwise at 0 ℃ under N_2 atmosphere. The mixture was stirred at room temperature for 4 h, the reaction was quenched by NH_4Cl aqueous, and extracted with CH_2Cl_2 (3 × 50 mL). The combined organic layers were then washed with brine, dried over anhydrous Na_2SO_4, and concentrated in vacuo to provide 1.8 g 5-acetylindole (**24**) as white solid. To a solution of **24** (500 mg, 3.14 mmol) in 20 mL anhydrous THF, NaH (60%, 188 mg, 4.71 mmol) was added and the mixture was stirred for 15 min. Then, $(Boc)_2O$ (822 mg, 4.71 mmol) was added dropwise. After stirring for 1 h, the mixture was diluted with 50 mL EtOAc, then washed with water (20 mL × 3), saturated brine, dried over anhydrous Na_2SO_4, and concentrated in vacuo to afford the crude product, which was purified by column chromatography with petroleum/ethyl acetate (5:1) to give intermediate **21a** (650 mg, 79.9%). The spectral data of **21c** was in accordance with literature report [36].

*4.1.5 The general procedure for the preparations of compounds **26a-d**.*

To the solutions of various acetylindoles (0.82 mmol) in 10 *p*-mL EtOH, toluenesulfonhydrazide (183 mg, 0.98 mmol) was added. After stirring for 2 h at refluxing temperature, the mixtures were cooled to room temperature, and the precipitates were collected by filtration, washed with cold EtOH and dried to afford corresponding *N*-tosylhydrazones **25a-c** as yellow solids in moderate to excellent yields. Then, to the solutions of **25a-c** (0.98 mmol) in 2 mL dioxane in sealed tube, 4-chlorine-2-methylquinoline (40 mg, 0.23 mmol), Xphos (19 mg, 0.04 mmol), $Pd(CH_3CN)_2Cl_2$ (6 mg, 0.02 mmol),*t*-BuOLi (40 mg, 0.51 mmol) were added. After stirring for 2 h at 90 ℃, the mixtures were filtered and the filtrates were concentrated to afford the crude products, which were purified by column chromatography with petroleum/ethyl acetate (5:1) to give compounds **26a-c** in good yields.

*4.1.5.1 4-(1-(6-methoxy-1H-indol-3-yl)vinyl)-2-methylquinoline (**26a**)*

Grey solid, yield 50.2%; ^{1}H NMR (300 MHz, $CDCl_3$) δ 8.41 (s, 1H), 8.02 (d, *J* = 8.5 Hz, 1H), 7.89 (d, *J* = 8.4 Hz, 1H), 7.76 (d, *J* = 8.6 Hz, 1H), 7.65 - 7.55 (m, 1H), 7.30 (s, 1H), 7.13 - 7.03 (m, 1H), 6.99 - 6.87 (m, 1H), 6.86 - 6.84 (m, 1H), 6.53 (d, *J* = 2.5 Hz, 1H), 6.05 (d, *J* = 1.4 Hz, 1H), 5.30 (d, *J* = 1.5 Hz, 1H), 3.84 (s, 3H), 2.75 (s, 3H); ^{13}C NMR (75 MHz, $CDCl_3$) δ 158.26, 156.13, 152.03, 149.51, 147.50, 139.73, 137.29, 128.80, 127.94, 125.78, 124.99, 123.72, 121.50, 120.65, 118.94, 116.80, 112.69, 109.90, 94.45, 55.13, 24.73; HR-MS (ESI) m/z: calcd for $C_{21}H_{19}N_2O$ $[M+H]^+$ 315.1492, found 315.1498.

*4.1.5.2 4-(1-(1H-indol-4-yl)vinyl)-2-methylquinoline (**26b**)*

Grey solid, yield 62.5%; ^{1}H NMR (300 MHz, $CDCl_3$) δ 8.54 (s, 1H), 8.04 (d, *J* = 8.4 Hz, 1H), 7.86 (dd, *J* = 8.3, 1.4 Hz, 1H), 7.59 (ddd, *J* = 8.3, 6.8, 1.4 Hz, 1H), 7.34 (d, *J* = 8.0 Hz, 1H), 7.30 (s, 1H), 7.25 (s, 1H), 7.17 (t, *J* = 2.8 Hz, 1H), 7.08 (s, 1H), 6.92 – 6.86 (m, 1H), 6.45 (s, 1H), 6.12 (d, *J* = 1.6 Hz, 1H), 5.66 (d, *J* = 1.6 Hz, 1H), 2.75 (s, 3H); ^{13}C NMR (75 MHz, $CDCl_3$) δ 158.19, 149.38, 145.70, 129.39, 128.73, 128.12, 127.32, 125.47, 125.10, 124.26, 122.17, 121.87, 121.17, 119.37, 119.07, 110.79, 101.56, 100.63, 100.11, 55.10; HR-MS (ESI) m/z: calcd for $C_{20}H_{17}N_2$ $[M+H]^+$ 285.1386, found 285.1388.

*4.1.5.3 tert-butyl 5-(1-(2-methylquinolin-4-yl)vinyl)-1H-indole-1-carboxylate (**26c**)*

Grey solid, yield 70.5%; ^{1}H NMR (300 MHz, $CDCl_3$) δ 8.01 (s, 1H), 7.98 (d, *J* = 2.7 Hz, 1H), 7.66 (d, *J* = 8.4 Hz, 1H), 7.61 - 7.54 (m, 1H), 7.51 (d, *J* = 3.8 Hz, 1H), 7.35 - 7.31 (m, 1H), 7.30 - 7.26 (m, 1H), 7.26 - 7.22 (m, 1H), 7.21 (d, *J* = 4.5 Hz, 1H), 6.40 (d, *J* = 3.7 Hz, 1H), 5.95 (s, 1H), 5.33 (s, 1H), 2.72 (s, 3H), 1.59 (s, 9H); ^{13}C NMR (75 MHz, $CDCl_3$) δ 158.29, 149.09, 148.45, 147.74, 146.04, 134.23, 130.24, 128.73, 128.36, 126.09, 125.61, 125.07, 124.95, 122.40, 122.05, 118.88, 115.68, 114.66, 106.97, 83.38, 27.67, 24.90; HR-MS (ESI) m/z: calcd for $C_{25}H_{25}N_2O_2$ $[M+H]^+$ 385.1911, found 385.1916.

*4.1.5.4 4-(1-(1H-indol-5-yl)vinyl)-2-methylquinoline (**26d**)*

To a solution of **26c** (75 mg, 0.20 mmol) in 10 mL CH_3OH, K_2CO_3 (33 mg, 0.24 mmol) was added. After stirring for 2 h at refluxing temperature, the mixture was extracted with CH_2Cl_2 (3 × 25 mL). The combined organic layers were then washed with brine, dried over anhydrous Na_2SO_4, and concentrated in vacuo to provide the crude product, which was purified by column chromatography with petroleum/ethyl acetate (5:1) to give 50 mg **26d** as grey solid, yield 90.9%; ^{1}H NMR (300 MHz, $CDCl_3$) δ 8.31 (s, 1H), 8.04 (d, *J* = 8.4 Hz, 1H), 7.79 (dd, *J* = 8.3, 1.4 Hz, 1H), 7.62 (ddd, *J* = 8.4, 6.8, 1.5 Hz, 1H), 7.51 - 7.44 (m, 1H), 7.34 - 7.31 (m, 1H), 7.31 - 7.29 (m, 1H), 7.29 (s, 1H), 7.23 (dd, *J* = 8.5, 1.7 Hz, 1H), 7.19 (t, *J* = 2.8 Hz, 1H), 6.47 – 6.45 (m, 1H), 5.98 (d, *J* = 1.2 Hz, 1H), 5.33 (d, *J* = 1.2 Hz, 1H), 2.78 (s, 3H); ^{13}C NMR (75 MHz, $CDCl_3$) δ 158.30, 149.24, 147.65, 146.57, 135.22, 131.48, 128.77, 128.08, 127.47, 125.87, 125.24, 125.07, 124.60, 122.10, 120.31, 118.86, 114.47, 110.66, 102.43, 24.80; HR-MS (ESI) m/z: calcd for $C_{20}H_{17}N_2$ $[M+H]^+$ 285.1386, found 285.1391.

*4.1.6 The general procedures for the preparations of compounds **27a-d**.*

To the solutions of **26a**, **26b** or **26d** (0.16 mmol) in 10 mL anhydrous THF, NaH (60%, 10 mg, 0.24 mmol) was added and the mixtures were stirred for 15 min. CH_3I or C_2H_5I (0.20 mmol) was added, after stirring for 30 min at ambient temperature, the mixtures were extracted with CH_2Cl_2 (3 × 25 mL). The combined organic layers were then washed with brine (25 mL), dried over anhydrous Na_2SO_4, and concentrated in

vacuo. The residues were purified by column chromatography with petroleum/ethyl acetate (5:1) an eluent to afford products **27a-d** as grey solids in good to excellent yields.

*4.1.6.1 4-(1-(6-methoxy-1-methyl-1H-indol-3-yl)vinyl)-2-methylquinoline (**27a**)*

Grey solid, yield 85.2%; ^{1}H NMR (300 MHz, $CDCl_3$) δ 8.05 (d, *J* = 8.5 Hz, 1H), 7.91 (d, *J* = 7.9 Hz, 1H), 7.78 (d, *J* = 8.7 Hz, 1H), 7.68 - 7.59 (m, 1H), 7.34 (d, *J* = 8.3 Hz, 1H), 7.30 (s, 1H), 6.88 (dd, *J* = 8.7, 2.3 Hz, 1H), 6.76 (d, *J* = 2.3 Hz, 1H), 6.40 (s, 1H), 6.02 (d, *J* = 1.3 Hz, 1H), 5.24 (d, *J* = 1.3 Hz, 1H), 3.90 (s, 3H), 3.58 (s, 3H), 2.78 (s, 3H); ^{13}C NMR (75 MHz, $CDCl_3$) δ 158.23, 156.07, 149.53, 147.54, 141.70, 139.60, 138.05, 128.79, 128.30, 128.06, 125.78, 125.00, 121.45, 120.88, 119.40, 115.38, 112.04, 109.47, 92.68, 55.21, 32.31, 24.82; HR-MS (ESI) m/z: calcd for $C_{22}H_{21}N_2O[M+H]^+$ 329.1648, found 329.1655.

*4.1.6.2 2-methyl-4-(1-(1-methyl-1H-indol-4-yl)vinyl) quinoline (**27b**)*

Yield 73.5%, grey solid; ^{1}H NMR (300 MHz, $CDCl_3$) δ 8.02 (d, *J* = 8.5 Hz, 1H), 7.84 (d, *J* = 8.8 Hz, 1H), 7.63 - 7.57 (m, 1H), 7.30 (s, 1H), 7.27 (s, 1H), 7.26 (s, 1H), 7.12 (t, *J* = 7.8 Hz, 1H), 7.02 (d, *J* = 3.1 Hz, 1H), 6.88 (d, *J* = 7.6 Hz, 1H), 6.38 (d, *J* = 3.2 Hz, 1H), 6.11 (d, *J* = 1.7 Hz, 1H), 5.65 (d, *J* = 1.7 Hz, 1H), 3.80 (s, 3H), 2.75 (s, 3H); ^{13}C NMR (75 MHz, $CDCl_3$) δ 158.17, 149.20, 147.81, 145.71, 136.69, 132.90, 128.69, 128.65, 128.53, 128.33, 125.62, 125.41, 125.05, 124.95, 121.82, 120.95, 119.13, 108.76, 100.22, 32.52, 24.89; HR-MS (ESI) m/z: calcd for $C_{22}H_{19}N_2[M+H]^+$ 299.1543, found 299.1544.

*4.1.6.3 2-methyl-4-(1-(1-methyl-1H-indol-5-yl)vinyl) quinoline (**27c**)*

Yield 83.4%, grey solid; ^{1}H NMR (300 MHz, $CDCl_3$) δ 8.05 (d, *J* = 8.4 Hz, 1H), 7.84 - 7.75 (m, 1H), 7.65 - 7.57 (m, 1H), 7.46 (s, 1H), 7.29 (s, 2H), 7.27 - 7.25 (m, 1H), 7.25 (s, 1H), 7.02 (d, *J* = 3.1 Hz, 1H), 6.38 (d, *J* = 3.1 Hz, 1H), 5.98 (s, 1H), 5.32 (s, 1H), 3.77 (s, 3H), 2.78 (s, 3H); ^{13}C NMR (75 MHz, $CDCl_3$) δ 158.25, 149.06, 147.72, 146.63, 136.00, 131.11, 129.06, 128.65, 128.26, 127.94, 125.79, 125.18, 124.97, 122.03, 119.94, 119.11, 114.35, 108.73, 101.02, 32.42, 24.91; HR-MS (ESI) m/z: calcd for $C_{21}H_{19}N_2[M+H]^+$ 299.1543, found 299.1543.

*4.1.6.4 2-methyl-4-(1-(1-ethyl-1H-indol-5-yl)vinyl) quinoline (**27d**)*

Yield 72.0%, white solid; ^{1}H NMR (300 MHz, $CDCl_3$) δ 7.94 (dd, *J* = 8.5, 1.2 Hz, 1H), 7.69 (d, *J* = 7.7 Hz, 1H), 7.47 (ddd, *J* = 8.4, 6.8, 1.5 Hz, 1H), 7.34 (s, 1H), 7.16 (s, 1H), 7.14 (s, 1H), 7.11 (s, 1H), 7.11 - 7.10 (m, 1H), 6.92 (d, *J* = 3.1 Hz, 1H), 6.25 (d, *J* = 3.2 Hz, 1H), 5.85 (d, *J* = 1.3 Hz, 1H), 5.18 (d, *J* = 1.2 Hz, 1H), 3.94 (t, *J* = 7.3 Hz, 2H), 2.65 (s, 3H), 1.27 (t, *J* = 7.3 Hz, 3H); ^{13}C NMR (75 MHz, $CDCl_3$) δ 158.25, 149.11, 147.71, 146.59, 135.04, 131.04, 128.67, 128.25, 128.11, 127.28, 125.83, 125.22, 125.00, 122.03, 119.79, 119.21, 114.28, 108.80, 101.15, 40.58, 24.91, 14.99; HR-MS (ESI) m/z: calcd for $C_{22}H_{21}N_2[M+H]^+$ 313.1699, found 313.1702.

*4.1.7 The general procedures for the preparations of compounds **28a-c**.*

To solutions of **26a**, **27b** or **27c** (0.16 mmol) in 10 mL anhydrous CH_3OH, Pd-C (5 mg) was added and the mixtures were stirred overnight under H_2 atmosphere. Then, the mixtures were filtered and the filtrates were concentrated. The residues were purified by column chromatography with petroleum/ethyl acetate (5:1) to give compounds **28a-c** in good yields.

*4.1.7.1 4-(1-(6-methoxy-1H-indol-3-yl)ethyl)-2-methylquinoline (**28a**)*

Yield 72.3%, white solid; ^{1}H NMR (300 MHz, $CDCl_3$) δ 8.23 (s, 1H), 8.10 (d, *J* = 8.6 Hz, 1H), 8.00 (d, *J* = 8.4 Hz, 1H), 7.59 (t, *J* = 7.7 Hz, 1H), 7.41 (t, *J* = 7.8 Hz, 1H), 7.08 (d, *J* = 8.8 Hz, 1H), 7.04 (s, 1H), 6.80 (s, 1H), 6.77 (s, 1H), 6.60 (d, *J* = 8.9 Hz, 1H), 5.04 (d, *J* = 7.2 Hz, 1H), 3.73 (s, 3H), 2.56 (s, 3H), 1.72 (d, *J* = 7.0 Hz, 3H); ^{13}C NMR (75 MHz, $CDCl_3$) δ 158.44, 156.05, 151.86, 147.67, 147.52, 136.92, 128.84, 128.42, 125.05, 124.84, 122.74, 120.50, 120.23, 119.41, 119.31, 108.83, 94.19, 55.11, 31.27, 24.96, 20.84; HR-MS (ESI) m/z: calcd for $C_{21}H_{21}N_2O[M+H]^+$ 317.1648, found
317.1655.

*4.1.7.2 2-methyl-4-(1-(1-methyl-1H-indol-4-yl) ethyl)quinolone (**28b**)*

Yield 60%, white solid; ^{1}H NMR (300 MHz, $CDCl_3$) δ 8.06 - 8.03 (m, 1H), 8.02 -7.99 (m, 1H), 7.60 (ddd, *J* = 8.4, 6.9, 1.4 Hz, 1H), 7.37 (ddd, *J* = 8.3, 6.8, 1.3 Hz, 1H), 7.22 (d, *J* = 9.6 Hz, 2H), 7.14 (t, *J* = 7.7 Hz, 1H), 7.02 (d, *J* = 3.1 Hz, 1H), 6.85 (d, *J* = 7.1 Hz, 1H), 6.42 (dd, *J* = 3.2, 0.9 Hz, 1H), 5.29 (q, *J* = 7.2 Hz, 1H), 3.79 (s, 3H), 2.69 (s, 3H), 1.82 (d, *J* = 7.1 Hz, 3H); ^{13}C NMR (75 MHz, $CDCl_3$) δ 158.26, 151.36, 147.69, 136.55, 136.23, 128.85, 128.65, 128.29, 128.15, 126.79, 125.07, 122.99, 121.28, 119.60, 116.72, 107.37, 98.55, 36.90, 32.49, 25.14, 20.50; HR-MS (ESI) m/z: calcd for $C_{21}H_{21}N_2[M+H]^+$ 301.1699, found 301.1702.

*4.1.7.3 2-methyl-5-(1-(1-methyl-1H-indol-4-yl) ethyl)quinolone (**28c**)*

Yield 70.3%, white solid; ^{1}H NMR (300 MHz, $CDCl_3$) δ 8.17 - 8.08 (m, 1H), 8.06 (d, *J* = 7.3 Hz, 1H), 7.62 (ddd, *J* = 8.4, 6.8, 1.4 Hz, 1H), 7.52 (s, 1H), 7.44 - 7.36 (m, 1H), 7.28 (s, 1H), 7.24 (d, *J* = 8.4 Hz, 1H), 7.10 (dd, *J* = 8.5, 1.7 Hz, 1H), 7.02 (d, *J* = 3.1 Hz, 1H), 6.44 (d, *J* = 3.1 Hz, 1H), 5.02 (q, *J* = 7.1 Hz, 1H), 3.73 (s, 3H), 2.77 (s, 3H), 1.83 (d, *J* = 7.1 Hz, 3H); ^{13}C NMR (75 MHz, $CDCl_3$) δ 158.23, 151.84, 147.80, 135.51, 135.06, 128.82, 128.70, 128.24, 128.17, 125.13, 124.94, 123.40, 121.30, 119.59, 118.82, 108.88, 100.32, 39.68, 32.31, 25.13, 22.01; HR-MS (ESI) m/z: calcd for $C_{21}H_{21}N_2[M+H]^+$ 301.1699, found 301.1705.

*4.1.8 The general procedures for the preparations of compounds **30a**, **30c**, **33a** and **33c**.*

To solutions of 5-methoylindole or 4-nitro-5-methoylindole (0.68 mmol) in 10 mL anhydrous DMF, NaH (60%, 41 mg, 1.02 mmol) was added under N_2 atmosphere and the mixtures were stirred for 15 min. Then, 4-chloride-2-methylquinoline or newly prepared 2-methylquinoline-4-formyl chloride (0.68 mmol) was added and the

mixtures were stirred overnight at 50 ℃. Then, the mixtures were diluted with 25 mL EtOAc, then washed with water (20 mL × 3), saturated brine, dried over anhydrous Na_2SO_4, and concentrated in vacuo, the residues were purified by column chromatography with petroleum/ethyl acetate (5:1) to give **30a**, **30b**, **33a** and **33b**; Then, compounds **30b** or **33b** (0.24 mmol) was dissolved into 5 mL mixture solvent of EtOH and AcOH (1:1), and Fe powder (134 mg, 2.4 mmol) was added in one potion. The reactions were stirred for 2 h at 65 ℃, then the solvents were removed in vavo and the residues were neutralized by saturated $NaHCO_3$ aqueous. The mixtureswere filtrated, and the filtrates were extracted with EtOAc (3 × 20 mL). The combined organic layers were then washed with saturated brine, dried over anhydrous Na_2SO_4, and concentrated in vacuo to afford the crude products, which were purified by column chromatography with petroleum/ethyl acetate (2:1) to give **30c** or **33c**. *4.1.8.1 4-(5-methoxy-1H-indol-1-yl)-2-methylquinoline (**30a**)*

Yield 25.5%, grey solid; ^{1}H NMR (300 MHz, $CDCl_3$) δ 9.87 (s, 1H), 8.20 (d, *J* = 3.1 Hz, 1H), 8.17 (d, *J* = 2.8 Hz, 1H), 8.12 (d, *J* = 2.3 Hz, 1H), 7.80 (d, *J* = 7.9 Hz, 1H), 7.74 (d, *J* = 8.1 Hz, 1H), 7.55 (t, *J* = 7.6 Hz, 1H), 7.48 (s, 1H), 7.40 (s, 1H), 7.12 (dd, *J* = 8.7, 2.4 Hz, 1H), 3.94 (s, 3H), 2.87 (s, 3H); ^{13}C NMR (75 MHz, $CDCl_3$) δ 185.53, 158.68, 152.70, 148.30, 135.30, 130.83, 129.63, 127.72, 127.10, 124.13, 123.49, 122.84, 122.23, 120.29, 119.01, 115.23, 100.63, 55.81, 29.69; HR-MS (ESI) m/z: calcd for $C_{19}H_{17}N_2O[M+H]^+$ 289.1335, found 289.1342.

*4.1.8.2 5-methoxy-1-(2-methylquinolin-4-yl)-1H-indol-4-amine (**30c**)*

Yield 20.4% over two steps, yellow oil; ^{1}H NMR (300 MHz, $CDCl_3$) δ 8.08 - 8.02 (m, 1H), 7.69 - 7.62 (m, 2H), 7.37 - 7.31 (m, 1H), 7.26 (s, 1H), 7.17 (d, *J* = 3.4 Hz, 1H), 6.75 (d, *J* = 8.8 Hz, 1H), 6.60 (d, *J* = 3.3 Hz, 1H), 6.48 (d, *J* = 8.8 Hz, 1H), 4.01 (s, 2H), 3.79 (s, 3H), 2.70 (s, 3H); ^{13}C NMR (75 MHz, $CDCl_3$) δ 159.50, 149.58, 144.72, 140.32, 133.61, 130.17, 129.06, 128.46, 128.30, 126.22, 123.66, 122.99, 119.05, 118.89, 110.27, 100.87, 100.39, 57.61, 25.39; HR-MS (ESI) m/z: calcd for $C_{19}H_{18}N_3O[M+H]^+$ 304.1444, found 304.1448.

*4.1.8.3 (5-methoxy-1H-indol-1-yl)(2-methylquinolin-4-yl)methanone (**33a**)*

Yield 39.4%, grey solid; ^{1}H NMR (300 MHz, $CDCl_3$) δ 8.48 (s, 1H), 8.16 (d, *J* = 8.2 Hz, 1H), 7.83 - 7.73 (m, 2H), 7.55 - 7.50 (m, 1H), 7.46 (s, 1H), 7.13 - 7.04 (m, 2H), 6.87 (s, 1H), 6.53 (d, *J* = 3.7 Hz, 1H), 3.92 (s, 3H), 2.85 (s, 3H); ^{13}C NMR (75 MHz, $CDCl_3$) δ 165.44, 158.07, 156.75, 147.65, 140.24, 131.55, 129.90, 129.72, 128.76, 126.84, 126.67, 124.12, 122.10, 119.69, 116.96, 113.19, 109.52, 103.60, 55.21, 24.84; HR-MS (ESI) m/z: calcd for $C_{20}H_{17}N_2O_2[M+H]^+$ 317.1285, found 317.1288.

*4.1.8.4 (4-amino-5-methoxy-1H-indol-1-yl)(2-methylquinolin-4-yl)methanone (**33c**)*

Yield 23.5% over two steps, yellow oil; ^{1}H NMR (300 MHz, $CDCl_3$) δ 8.17 - 8.07 (m, 1H), 7.94 (s, 1H), 7.76 (d, *J* = 6.9 Hz, 1H), 7.73 (s, 1H), 7.50 (d, *J* = 8.2 Hz, 1H),

7.44 (d, *J* = 9.6 Hz, 1H), 6.98 (d, *J* = 8.8 Hz, 1H), 6.75 (s, 1H), 6.49 (s, 1H), 4.12 (s, 2H), 3.95 (s, 3H), 2.83 (s, 3H); ^{13}C NMR (75 MHz, $CDCl_3$) δ 166.01, 158.62, 148.15, 143.52, 140.99, 131.08, 130.37, 129.25, 128.41, 127.12, 125.70, 124.69, 122.59, 120.14, 119.56, 110.03, 106.57, 106.40, 56.66, 25.42; HR-MS (ESI) m/z: calcd for $C_{20}H_{18}N_3O_2[M+H]^+$ 332.1394, found 332.1393.

*4.1.9 The synthesis of 4-(1-(1-(fluoromethyl)-1H-indol-5-yl)vinyl)-2-methylquinoline (**34a**).* $ClCH_2F$ gas was inlet to a solution of 5 mL DMF in sealed tube under ice-bath condition for 5 min, then NaH (60%, 28 mg, 0.70 mmol) and **26d** (100 mg, 0.36 mmol) were added. The mixture was stirred at 80 ℃ for 2 h, which was then diluted with 25 mL EtOAc, washed with water (20 mL × 3), saturated brine, dried over anhydrous Na_2SO_4, and concentrated in vacuo, and the residue was purified by flash column chromatography with petroleum/ethyl acetate (5:1) to give the product **34a** as white solid, which was unstable in the silicagel column leading to low yield 18.0%;
^{1}H NMR (300 MHz, $CDCl_3$) δ 8.05 (d, *J* = 8.4 Hz, 1H), 7.75 (dd, *J* = 8.4, 1.4 Hz, 1H), 7.62 (ddd, *J* = 8.5, 6.9, 1.4 Hz, 1H), 7.45 (d, *J* = 1.6 Hz, 1H), 7.40 (d, *J* = 8.6 Hz, 1H), 7.36 - 7.29 (m, 2H), 7.28 (s, 1H), 7.16 (d, *J* = 3.4 Hz, 1H), 6.52 - 6.46 (m, 1H), 6.17 (s, 1H), 5.99 (d, *J* = 2.6 Hz, 2H), 5.37 (d, *J* = 1.1 Hz, 1H), 2.78 (s, 3H); ^{13}C NMR (75 MHz, $CDCl_3$) δ 158.30, 148.67, 147.69, 146.18, 129.10, 128.77, 128.28, 128.20, 128.15, 125.67, 125.10, 122.08, 121.30, 119.36, 115.30, 108.95, 104.77, 104.74, 84.66, 82.03, 24.90; HR-MS (ESI) m/z: calcd for $C_{21}H_{18}FN_2[M+H]^+$ 317.1449, found 329.1452.

*4.1.10 The synthesis of (5-(1-(2-methylquinolin-4-yl)vinyl)-1H-indol-1-yl)methanol (**34b**).* To a solution of **26d** (70 mg, 0.25 mmol) in 2 mL EtOH, 1 mL 10% NaOH aqueous and 1 mL formaldehyde aqueous were added. The mixture was stirred for 2 h, and the precipitates were collected by filtration, washed with water and dried to afford **34b** as pink solid (50 mg, yield 64.9%); ^{1}H NMR (300 MHz, DMSO-d_6) δ 7.95 (d, *J* = 8.3 Hz, 1H), 7.70 - 7.57 (m, 2H), 7.52 (d, *J* = 8.4 Hz, 1H), 7.37 (s, 2H), 7.32 (s, 1H), 7.25 (s, 1H), 6.39 (d, *J* = 23.4 Hz, 2H), 6.01 (s, 1H), 5.49 (d, *J* = 6.8 Hz, 2H), 5.31 (s, 1H), 3.35 (s, 1H), 2.70 (s, 3H); ^{13}C NMR (75 MHz, DMSO-d_6) δ 158.66, 148.54, 147.62, 146.63, 135.22, 131.26, 129.26, 129.07, 128.62, 128.57, 125.71, 125.47, 124.84, 122.22, 119.77, 118.66, 114.90, 110.57, 101.70, 68.63, 24.79; HR-MS (ESI) m/z: calcd for $C_{21}H_{19}N_2O[M+H]^+$ 315.1492, found 315.1497.

*4.1.11 The synthesis of 1-((1-(2-methylquinolin-4-yl)vinyl)-1H-indol-1-yl)ethan-1-one (**34c**).* To a solution of **26d** (50 mg, 0.18 mmol) in 5 mL DCM, glacial acetic acid (22 μL, 0.21 mmol), Et_3N (36 μL, 0.54 mmol) and catalytic DMAP were added. The mixture was refluxed overnight, which were then diluted with 25 mL EtOAc, washed with water (20 mL × 3), saturated brine, dried over anhydrous Na_2SO_4, and

concentrated in vacuo. The residue was purified by flash column chromatography with petroleum/ethyl acetate (5:1) to give the product **34c** as white solid (45 mg, 78.9%); ^{1}H NMR (300 MHz, $CDCl_3$) δ 8.37 (d, *J* = 8.7 Hz, 1H), 8.05 (d, *J* = 8.1 Hz, 1H), 7.70 (d, *J* = 8.4 Hz, 1H), 7.62 (ddd, *J* = 8.4, 6.9, 1.5 Hz, 1H), 7.42 (dd, *J* = 8.7, 1.9 Hz, 1H), 7.37 (d, *J* = 3.7 Hz, 1H), 7.34 (d, *J* = 1.7 Hz, 1H), 7.30 (d, *J* = 7.1 Hz, 1H), 7.28 (s, 1H), 6.51 (d, *J* = 4.0 Hz, 1H), 6.03 (d, *J* = 1.1 Hz, 1H), 5.41 (d, *J* = 1.1 Hz, 1H), 2.78 (s, 3H), 2.61 (s, 3H); ^{13}C NMR (75 MHz, $CDCl_3$) δ 168.00, 158.30, 148.30, 147.72, 145.85, 139.98, 135.16, 134.75, 130.11, 128.78, 128.35, 125.56, 125.37, 125.11, 124.91, 123.17, 122.06, 118.83, 116.08, 108.82, 24.88, 23.39; HR-MS (ESI) m/z: calcd for $C_{22}H_{19}N_2O[M+H]^+$ 327.1492, found 327.1496.

*4.1.12 The synthesis of 4-(1-(1-methyl-1H-indol-5-yl)vinyl)quinoline-2-carbaldehyde (**35a**).* To a solution of **27c** (100 mg, 0.34 mmol) in 5 mL dioxane, SeO_2 (45 mg, 0.4 mmol) was added. The mixture was refluxed for 2 h, which were then diluted with 25 mL EtOAc, washed with water (20 mL × 3), saturated brine, dried over anhydrous Na_2SO_4, and concentrated in vacuo. Then, the residue was purified by flash column chromatography with petroleum/ethyl acetate (20:1) to give the product **35a** as white solid (40 mg, 38.5%); ^{1}H NMR (300 MHz, $CDCl_3$) δ 10.29 (s, 1H), 8.27 (d, *J* = 8.2 Hz, 1H), 8.03 (s, 1H), 7.93 - 7.85 (m, 1H), 7.75 (ddd, *J* = 8.4, 6.9, 1.4 Hz, 1H), 7.52 - 7.43 (m, 1H), 7.41 (t, *J* = 1.2 Hz, 1H), 7.25 (d, *J* = 5.6 Hz, 1H), 7.23 (d, *J* = 1.6 Hz, 1H), 7.03 (d, *J* = 3.1 Hz, 1H), 6.37 (d, *J* = 3.1 Hz, 1H), 6.03 (d, *J* = 1.0 Hz, 1H), 5.37 (d, *J* = 1.1 Hz, 1H), 3.78 (s, 3H); ^{13}C NMR (75 MHz, $CDCl_3$) δ 193.51, 151.88, 150.64, 147.82, 146.23, 136.08, 130.77, 130.08, 129.64, 129.19, 128.78, 128.44, 127.99, 126.25, 119.89, 119.13, 117.46, 115.35, 108.88, 101.04, 32.43; HR-MS (ESI) m/z: calcd for $C_{21}H_{16}N_2NaO[M+Na]^+$ 335.1155, found 335.1155.

*4.1.13 The synthesis of (4-(1-(1-methyl-1H-indol-5-yl)vinyl)quinolin-2-yl)methanol (**35b**).* To a solution of **35a** (20 mg, 0.06 mmol) in 10 mL THF, $NaBH_4$ (4.8 mg, 0.12 mmol) was added. The mixture was stirred for 30 min, which were then quenched with NH_4Cl aqueous, diluted with 25 mL EtOAc, washed with water (20 mL × 3), saturated brine, dried over anhydrous Na_2SO_4, and concentrated in vacuo. The residue was purified by flash column chromatography with petroleum/ethyl acetate (2:1) to give the product **35b** as colorless oil (15 mg, 75%); ^{1}H NMR (300 MHz, $CDCl_3$) δ 8.10 (d, *J* = 8.9 Hz, 1H), 7.82 (dd, *J* = 8.4, 1.4 Hz, 1H), 7.65 (ddd, *J* = 8.4, 6.9, 1.4 Hz, 1H), 7.43 (s, 1H), 7.34 (ddd, *J* = 8.3, 6.9, 1.3 Hz, 1H), 7.27 (s, 1H), 7.26 – 7.23 (m, 2H), 7.02 (d, *J* = 3.1 Hz, 1H), 6.38 (d, *J* = 3.1 Hz, 1H), 5.99 (d, *J* = 1.2 Hz, 1H), 5.33 (d, *J* = 1.2 Hz, 1H), 4.95 (s, 2H), 3.77 (s, 3H); ^{13}C NMR (75 MHz, $CDCl_3$) δ 158.14, 150.01, 146.62, 145.55, 136.70, 132.66, 129.01, 128.79, 128.30, 126.08, 125.72,

125.65, 125.60, 120.96, 119.46, 119.14, 118.17, 108.88, 100.14, 63.62, 32.54; HR-MS (ESI) m/z: calcd for $C_{21}H_{19}N_2O[M+H]^+$ 315.1492, found 335.1494.

4.1.14 *The general procedures for the preparations of compounds **35c-g** and **35i***

Various C-2 substituted 4-chlorinequinolines were synthesized according to the literature report [27]. To the solution of *N*-tosylhydrazone **37** (150 mg, 0.44 mmol) in 2 mL dioxane in sealed tube, various 4-chlorinequinolines (0.44 mmol), Xphos (19 mg, 0.04 mmol), $Pd(CH_3CN)_2Cl_2$ (6 mg, 0.02 mmol), *t*-BuOLi (77 mg, 0.97 mmol) were added. After stirring for 2 h at 90 ℃, the mixtures were filtered and the filtrates were concentrated to afford the crude products, which were purified by column chromatography with petroleum/ethyl acetate (5:1) to give compounds **35c-g** and **35i** in good yields.

*4.1.14.1 N, N-dimethyl-4-(1-(1-methyl-1H-indol-5-yl)vinyl)quinolin-2-amine (**35c**)*

Yield 80%, yellow solid; ^{1}H NMR (300 MHz, $CDCl_3$) δ 7.72 (d, *J* = 8.2 Hz, 1H), 7.54 (dd, *J* = 8.1, 1.5 Hz, 1H), 7.51 (dd, *J* = 1.7, 0.7 Hz, 1H), 7.44 (ddd, *J* = 8.4, 6.9, 1.5 Hz, 1H), 7.31 (dd, *J* = 8.7, 1.8 Hz, 1H), 7.21 (s, 1H), 7.01 (d, *J* = 3.1 Hz, 1H), 7.00 - 6.93 (m, 1H), 6.90 (s, 1H), 6.37 (dd, *J* = 3.2, 0.9 Hz, 1H), 5.93 (d, *J* = 1.4 Hz, 1H), 5.31 (d, *J* = 1.4 Hz, 1H), 3.76 (s, 3H), 3.25 (s, 6H); ^{13}C NMR (75 MHz, $CDCl_3$) δ 157.10, 149.94, 148.05, 147.49, 136.03, 131.02, 128.99, 128.71, 127.99, 126.01, 125.79, 121.43, 121.03, 119.91, 119.07, 113.49, 109.07, 108.71, 101.06, 37.63, 32.41; HR-MS (ESI) m/z: calcd for $C_{22}H_{22}N_3[M+H]^+$ 328.1808, found 328.1814.

*4.1.14.2 2-methoxy-4-(1-(1-methyl-1H-indol-5-yl)vinyl)quinoline (**35d**)*

Yield 66.7%, White solid; ^{1}H NMR (300 MHz, $CDCl_3$) δ 7.90 – 7.83 (m, 1H), 7.65 (dd, *J* = 8.2, 1.4 Hz, 1H), 7.57 - 7.50 (m, 1H), 7.51 - 7.48 (m, 1H), 7.27 (dd, *J* = 8.7, 1.7 Hz, 1H), 7.21 (d, *J* = 0.9 Hz, 1H), 7.19 - 7.11 (m, 1H), 6.98 (d, *J* = 3.1 Hz, 1H), 6.94 (s, 1H), 6.36 (dd, *J* = 3.1, 0.8 Hz, 1H), 5.93 (d, *J* = 1.3 Hz, 1H), 5.31 (d, *J* = 1.3 Hz, 1H), 4.11 (s, 3H), 3.71 (s, 3H); ^{13}C NMR (75 MHz, $CDCl_3$) δ 161.86, 151.67, 146.59, 146.48, 136.05, 130.81, 129.03, 128.74, 127.99, 126.91, 126.00, 124.05, 123.31, 119.90, 119.03, 114.21, 112.78, 108.75, 101.06, 52.89, 32.40; HR-MS (ESI) m/z: calcd for $C_{21}H_{19}N_2O[M+H]^+$ 315.1492, found315.1493.

*4.1.14.3 N-methyl-4-(1-(1-methyl-1H-indol-5-yl)vinyl)quinolin-2-amine (**35e**)*

Yield 45.1%, White solid; ^{1}H NMR (300 MHz, $CDCl_3$) δ 7.72 (dd, *J* = 8.4, 1.2 Hz, 1H), 7.56 (dd, *J* = 8.2, 1.5 Hz, 1H), 7.51 (d, *J* = 1.7 Hz, 1H), 7.49 - 7.42 (m, 1H), 7.30 (dd, *J* = 8.6, 1.7 Hz, 1H), 7.25 (s, 1H), 7.22 (d, *J* = 8.7 Hz, 1H), 7.06 - 6.94 (m, 2H), 6.64 (s, 1H), 6.38 (d, *J* = 3.0 Hz, 1H), 5.92 (d, *J* = 1.4 Hz, 1H), 5.30 (d, *J* = 1.3 Hz, 1H), 3.75 (s, 3H), 3.11 (d, *J* = 4.9 Hz, 3H); ^{13}C NMR (75 MHz, $CDCl_3$) δ 156.96, 150.09, 147.81, 146.90, 136.01, 130.87, 128.96, 128.79, 127.94, 125.88, 125.66, 122.31, 121.36, 119.88, 119.01, 113.64, 110.91, 108.66, 101.04, 32.40, 28.26; HR-MS (ESI) m/z: calcd for $C_{21}H_{20}N_3[M+H]^+$ 314.1652, found 314.1655.

*4.1.14.4 4-(1-(1-methyl-1H-indol-5-yl)vinyl)quinolone (**35f**)*

Yield 64.7%, White solid; ^{1}H NMR (300 MHz, $CDCl_3$) δ 8.85 (d, *J* = 4.4 Hz, 1H), 8.05 (dd, *J* = 8.6, 1.3 Hz, 1H), 7.75 (dd, *J* = 8.5, 1.4 Hz, 1H), 7.55 (ddd, *J* = 8.4, 6.8, 1.5 Hz, 1H), 7.35 (d, *J* = 1.1 Hz, 1H), 7.29 (d, *J* = 4.4 Hz, 1H), 7.27 - 7.20 (m, 1H), 7.17 (d, *J* = 10.1 Hz, 1H), 7.14 (s, 1H), 6.91 (d, *J* = 3.1 Hz, 1H), 6.28 (d, *J* = 3.1 Hz, 1H), 5.90 (d, *J* = 1.2 Hz, 1H), 5.24 (d, *J* = 1.2 Hz, 1H), 3.65 (s, 3H); ^{13}C NMR (75 MHz, $CDCl_3$) δ 149.70, 149.14, 147.97, 146.52, 136.04, 131.04, 129.12, 129.05, 128.72, 127.98, 126.91, 126.06, 125.88, 121.27, 119.92, 119.12, 114.61, 108.80, 101.05, 32.41; HR-MS (ESI) m/z: calcd for $C_{21}H_{17}N_2[M+H]^+$ 285.1386, found 285.1391.

*4.1.14.5 4-(1-(1-methyl-1H-indol-5-yl)vinyl)quinoline-2-carbonitrile (**35g**)*

Yield 40.7%, White solid; ^{1}H NMR (300 MHz, $CDCl_3$) δ 8.19 (d, *J* = 8.7 Hz, 1H), 7.89 (d, *J* = 7.8 Hz, 1H), 7.79 - 7.73 (m, 1H), 7.69 (s, 1H), 7.52 - 7.45 (m, 1H), 7.39 (d, *J* = 1.0 Hz, 1H), 7.26 (s, 1H), 7.20 (dd, *J* = 8.6, 1.7 Hz, 1H), 7.05 (d, *J* = 3.1 Hz, 1H), 6.39 (dd, *J* = 3.2, 0.9 Hz, 1H), 6.05 (d, *J* = 0.8 Hz, 1H), 5.36 (d, *J* = 0.9 Hz, 1H), 3.79 (s, 3H); ^{13}C NMR (75 MHz, $CDCl_3$) δ 151.04, 148.10, 145.27, 136.15, 133.03, 130.36, 129.68, 129.40, 128.99, 128.65, 128.02, 127.55, 126.05, 123.33, 119.79, 119.18, 117.21, 115.88, 109.04, 101.09, 32.47; HR-MS (ESI) m/z: calcd for $C_{21}H_{16}N_3[M+H]^+$ 310.1339, found 310.1340.

*4.1.14.6 4-(1-(1-methyl-1H-indol-5-yl)vinyl)-2-(trifluoromethyl)quinolone (**35i**)*

Yield 57.0%, White solid; ^{1}H NMR (300 MHz, $CDCl_3$) δ 8.26 (d, *J* = 8.5 Hz, 1H), 7.92 (d, *J* = 8.5 Hz, 1H), 7.79 - 7.75 (m, 1H), 7.74 (d, *J* = 4.1 Hz, 1H), 7.47 (ddd, *J* = 8.0, 6.6, 1.2 Hz, 1H), 7.44 - 7.40 (m, 1H), 7.25 (d, *J* = 2.5 Hz, 1H), 7.05 (d, *J* = 3.1 Hz, 1H), 6.41 (d, *J* = 3.1 Hz, 1H), 6.06 (s, 1H), 5.39 (s, 1H), 5.30 (s, 1H), 3.79 (s, 3H); ^{13}C NMR (75 MHz, $CDCl_3$) δ 151.58, 147.48, 147.09, 147.02, 145.99, 136.12, 130.58, 129.95, 129.76, 129.28, 128.01, 127.81, 127.59, 126.01, 125.49, 123.02, 119.84, 119.16, 116.83, 116.80, 115.50, 108.95, 101.09, 32.43; HR-MS (ESI) m/z: calcd for $C_{21}H_{16}N_3O_2[M+H]^+$ 353.1260, found 353.1266.

4.1.15 *The synthesis of 4-(1-(1-methyl-1H-indol-5-yl)vinyl)quinoline-2-carboxamide (**35h**).* To a solution of *N*-tosylhydrazone **37** (118 mg, 0.34 mmol) in 2 mL dioxane in sealed tube, 4-chlorine-2-cyanquinoline (80 mg, 0.34 mmol), Xphos (17 mg, 0.03 mmol), $Pd(CH_3CN)_2Cl_2$ (9 mg, 0.03 mmol), *t*-BuOLi (87 mg, 1.09 mmol) were added. After stirring for 2 h at 90 ℃, the mixture was filtered and the filtrate was concentrated, the residue was purified by column chromatography with petroleum/ethyl acetate (5:1) to give 34 mg product **35h** as white solid, yield 30.0%;

^{1}H NMR (300 MHz, $CDCl_3$) δ 8.24 (s, 1H), 8.11 (d, *J* = 5.0 Hz, 1H), 8.04 (d, *J* = 8.5 Hz, 1H), 7.78 (d, *J* = 9.0 Hz, 1H), 7.64 - 7.57 (m, 1H), 7.34 (t, *J* = 1.2 Hz, 1H), 7.34 - 7.27 (m, 1H), 7.16 (d, *J* = 8.2 Hz, 2H), 6.93 (d, *J* = 3.1 Hz, 1H), 6.28 (d, *J* = 3.1 Hz, 1H), 5.98 (s, 1H), 5.96 - 5.89 (m, 1H), 5.29 (s, 1H), 3.67 (s, 3H); ^{13}C NMR (75 MHz,

$CDCl_3$) δ 166.70, 150.70, 148.56, 146.54, 136.04, 130.99, 129.49, 129.27, 129.08, 128.01, 127.34, 126.10, 119.98, 119.13, 118.93, 115.27, 108.80, 107.66, 101.02, 98.47, 32.42; HR-MS (ESI) m/z: calcd for $C_{21}H_{17}N_3NaO[M+Na]^+$ 350.1264, found 350.1267.

4.2 Pharmacology

4.2.1 In vitro antiproliferative assay

Cells were purchased from Nanjing KeyGen Biotech Co. Ltd. (Nanjing, China). The cytotoxicity of the test compounds was determined using the MTT assay. Briefly, the cell lines were incubated at 37 °C in a humidified 5% CO_2 incubator for 24 h in 96-microwell plates. After medium removal, 100 mL of culture medium with 0.1% DMSO containing the test compounds at different concentrations was added to each well and incubated at 37 °C for another 72 h. The MTT (5 mg/mL in PBS) was added and incubated for another 4 h, the optical density was detected with a microplate reader at 490 nm. The IC_{50} values were calculated according to the dose-dependent curves. All the experiments were repeated in at least three independent experiments.

4.2.2 In vitro tubulin polymerization inhibitory assay

An amount of 2 mg/mL tubulin (Cytoskeleton) was resuspended in PEM buffer containing 80 mM piperazine-N,N'-bis(2-ethanesulfonic acid) sequisodium salt PIPES (pH 6.9), 0.5 mM EGTA, 2 mM $MgCl_2$, and 15% glycerol. Then the mixture was preincubated with tested compounds or vehicle DMSO on ice. PEG containing GTP was added to the final concentration of 3 mg/mL before detecting the tubulin polymerization reaction. After 30 min, the absorbance was detected by a spectrophotometer at 340 nm at 37 °C every 2 min for 60 min. The area under the curve was used to determine the concentration that inhibited tubulin polymerization by 50% (IC_{50}), which was calculated with GraphPad Prism Software version 5.02.

4.2.3 Competitive Inhibition Assays.

The competitive binding activity of tested compounds was evaluated using a radiolabeled [3H] colchicine competition scintillation proximity (SPA) assay. In brief, 0.08 μM [3H] colchicine was mixed with **27c** (1 μM, 5 μM), **34b** (1 μM, 5 μM) or CA-4 (1 μM, 5 μM) and biotinylated porcine tubulin (0.5 μg) in a buffer of 100 μL containing 80 mM PIPES (pH 6.8), 1 mM EGTA, 10% glycerol, 1 mM $MgCl_2$, and 1 mM GTP for 2 h at 37 °C. Then streptavidin-labeled SPA beads (80 μg) were added to each mixture. The radioactive counts were measured directly with a scintillation counter.

4.2.4 Immunofluorescence Staining

K562 cells were seeded into 6-well plates and then treated with vehicle control 0.1% DMSO, **34b** (1, 2, 4 nM). The cells were fixed with 4% paraformaldehyde and then penetrated with PBS for three times. After blocking for 20 min by adding 50-100 μL goat serum albumin at room temperature, cells were incubated with a monoclonal antibody (anti-α-tubulin) at 37 °C for 2 h. Then the cells were washed three times by PBS following staining by fluorescence antibody and labeling of nuclei by 4,6-diamidino-2-phenylindole (DAPI). Cells were finally visualized using an LSM 570 laser confocal microscope (Carl Zeiss, Germany).

4.2.5 Cell cycle analysis

K562 cells were seeded into 6-well plates and incubated at 37 °C in a humidified 5% CO_2 incubator for 24 h, and then treated with or without **34b** at indicated concentrations for another 48 h. The collected cells were fixed by adding 70% ethanol at 4 °C for 12 h. Subsequently, the cells were resuspended in PBS containing 100 mL RNase A and 400 mL of propidium iodide for 30 min. The DNA content of the cells was measured using a FACS Calibur flow cytometer (Bectone Dickinson, San Jose, CA, USA).

4.2.6 Cell apoptosis analysis

After treatment with or without **34b** at indicated concentrations for 48 h, the cells were washed twice in PBS, centrifuged and resuspended in 500 mL AnnexinV binding buffer. The cells were then harvested, washed and stained with 5 mL Annexin V-APC and 5 mL 7-AAD in the darkness for 15 min. Apoptosis was analyzed using a FACS Calibur flow cytometer (Bectone Dickinson, San Jose, CA, USA).

4.2.7 Wound healing assay

K562 cells were grown in 6-well plates for 24 h. Scratches were made in confluent monolayers using 200 μL pipette tip. Then, wounds were washed twice with PBS to remove non-adherent cell debris. The media containing different concentrations (1, 2, 4 nM) of the compound **34b** were added to the petridishes. Cells which migrated across the wound area were photographed using phase contrast microscopy at 0 h and 24 h. The migration distance of cells migrated in to the wound area was measured manually.

4.2.8 Tube formation assay

EC Matrigel matrix was thawed at 4 °C overnight, and HUVECs suspended in DMEM were seeded in 96-well culture plates at a cell density of 50,000 cells/well after polymerization of the Matrigel at 37 °C for 30 min. They were then treated with 20 μL different concentrations of compound **34b** or vehicle for 6 h at 37 °C. Then, the

morphological changes of the cells and tubes formed were observed and photographed under inverted microscope (OLYMPUS, Japan).

4.2.9 In vivo antitumor evaluation

Five-week-old male Institute of Cancer Research (ICR) mice were purchased from Shanghai SLAC Laboratory Animals Co. Ltd. A total of 1×10^6 H22 cells were subcutaneously inoculated into the right flank of ICR mice according to protocols of tumor transplant research, to initiate tumor growth. After incubation for one day, mice were weighted and at random divided into eight groups of eight animals. The groups treated with **27c** and **34b** were administered 10, 20 mg/kg in a vehicle of 10% DMF/2% Tween 80/88% saline, respectively. The positive control group was treated with PTX (6 mg/kg) every 2 days by intravenous injection. CA-4 and CA-4P were administered 20 mg/kg in a vehicle of 10% DMF/2% Tween 80/88% saline and saline solution, respectively. The negative control group received a vehicle of 10% DMF/2% Tween 80/88% saline through intravenous injection. Treatments of **27c**, **34b**, CA-4 and CA-4P were done at a frequency of intravenous injection one dose per day for a total 21 consecutive days while the positive group was treated with PTX one dose per two days. The mice were sacrificed after the treatments and the tumors were excised and weighed. The inhibition rate was calculated as follows: Tumor inhibitory ratio (%) = (1-average tumor weight of treated group/average tumor weight of control group) × 100%.

4.3 Molecular modeling

In our study, the X-ray structure of the CA-4-*α,β*-tubulin complex was downloaded from the Protein Data Bank (PDB code 5lyi). The protein was prepared by removal of the stathmin-like domain, subunits C and D, water molecules and colchicine using Discovery Studio modules. The docking procedure was performed by employing DOCK program in Discovery Studio 3.0 software, and the structural image was obtained using PyMOL software.

Acknowledgments

The authors acknowledge the National Natural Science Foundation of China (No. 81373280; 81673306, 81703348), The Open Project of State Key Laboratory of Natural Medicines, China Pharmaceutical University (No. SKLNMKF 201710) for financial support, "Double First-Class" University project CPU2018GY04, China Pharmaceutical University.

REFERENCES

1. G. R. Pettit, S. B. Singh, E. Hamel, C. M. Lin, D. S. Alberts, D. Garcia-Kendal, Isolation and structure of the strong cell growth and tubulin inhibitor combretastatin A-4. Experiential. 45 (1989) 209-211.
2. C. M. Lin, S. B. Singh, P. S. Chu, R. O. Dempcy, J. M. Schmidt, G. R. Pettit, E. Hamel, Interactions of tubulin with potent natural and synthetic analogs of the antimitotic agent combretastatin: a structure-activity study. Mol. Pharmacol. 34 (1988) 200-208.
3. A. T. Mc Gown, B. W. Fox, Differential cytotoxicity of combretastatins A1 and A4 in two daunorubicin-resistant P388 cell lines. Cancer Chemother. Pharmacol. 26 (1990) 79-81.
4. G. G. Dark, S. A. Hill, V. E. Prise, G. M. Tozer, G. R. Pettit, D. J. Chaplin, Combretastatin A-4, an agent that displays potent and selective toxicity toward tumor vasculature. Cancer Res. 57 (1997) 1829-1834.
5. http://investor.mateon.com/releasedetail.cfm?ReleaseID=1041745.
6. S. Aprile, E. Del Grosso, G. C. Tron, G. Grosa, Identification of the human UDP-glucuronosyltransferases involved in the glucuronidation of combretastatin A-4. Drug Metab. Dispos. 35 (2007) 2252-2261.
7. S. Aprile, E. Del Grosso, G. C. Tron, G. Grosa, In vitro metabolism study of combretastatin A-4 in rat and human liver microsomes. Drug Metab. Dispos. 35 (2007) 2252-2261.
8. G. R. Pettit, B. Toki, D. L. Herald, P. Verdier-Pinard, M. R. Boyd, E. Hamel, R. K. Pettit, Antineoplastic agents. 379. synthesis of phenstatin phosphate. J. Med. Chem. 41 (1998) 1688-1695.
9. S. Messaoudi, B. Tréguier, A. Hamze, O. Provot, J. F. Peyrat, J. R. Rodrigo De Losada, J. M. Liu, J. Bignon, J. Wdzieczak-Bakala, S. Thoret, J. Dubois, J. D. Brion, M. Alami, Isocombretastatins a versus combretastatins A: the forgotten isoCA-4 isomer as a highly promising cytotoxic and antitubulin agent. J. Med. Chem. 52 (2009) 4538-4542.
10. M. A. Soussi, S. Aprile, S. Messaoudi, O. Provot, E. Del Grosso, J. Bignon, J. Dubois, J. D. Brion, G. Grosa, M. Alami, The metabolic fate of isoCombretastatin A-4 in human liver microsomes: identification, synthesis and biological evaluation of metabolites. ChemMedChem 6 (2011) 1781-1788.
11. M. Sriram, J. J. Hall, N. C. Grohmann, T. E. Strecker, T. Wootton, A. Franken, M. L. Trawick, K. G. Pinney, Design, synthesis and biological evaluation of dihydronaphthalene and benzosuberene analogs of the combretastatins as inhibitors of tubulin polymerization in cancer chemotherapy. Bioorg. Med. Chem. 16 (2008) 8161-8171.
12. C. A. Herdman, T. E. Strecker, R. P. Tanpure, Z. Chen, A. Winters, J. Gerberich, L. Liu, E. Hamel, R. P. Mason, D. J. Chaplin, M. L. Trawick, K. G. Pinney, Synthesis and biological evaluation of benzocyclooctene-based and indene-based anticancer agents that function as inhibitors of tubulin polymerization. Med. Chem. Comm. 7 (2012) 2418-2427.
13. E. Rasolofonjatovo, O. Provot, A. Hamze, J. Rodrigo, J. Bignon, J. Wdzieczak-Bakala, D. Destravines, J. Dubois, J. Brion, M. Alami, Conformationnally restricted naphthalene derivatives type isocombretastatin A-4 and isoerianin analogues: synthesis, cytotoxicity and

antitubulin activity. Eur. J. Med. Chem. 52 (2012) 22-32.

14. U. Galli, C. Travelli, S. Aprile, E. Arrigoni, S. Torretta, G. Grosa, A. Massarotti, G. Sorba, P. L. Canonico, A. A. Genazzani, G. C. Tron, Design, synthesis, and biological evaluation of combretabenzodiazepines: a novel class of anti-tubulin agents. J. Med. Chem. 58 (2015) 1345-1357.
15. T. Naret, J. Bignon, G. Bernadat, M. Benchekroun, H. Levaique, C. Lenoir, J. Dubois, A. Pruvost, F. Saller, D. Borgel, B. Manoury, V. Leblais, R. Darrigrand, S. Apcher, J. Brion, E. Schmitt, F. R. Leroux, M. Alami, A. Hamze, A fluorine scan of a tubulin polymerization inhibitor isocombretastatin A-4: Design, synthesis, molecular modelling, and biological evaluation. Eur. J. Med. Chem. 143 (2018) 473-490.
16. R. Álvarez, L. Aramburu, P. Puebla, E. González, M. Vicente, M. Medarde, R. Peláez, Pyridine based antitumour compounds acting at the colchicine site. Curr. Med. Chem. 23 (2016) 1100-1130.
17. W. Li, H. Sun, S. Sun, Z. Zhu, J. Xu, Tubulin inhibitors targeting the colchicine binding site: a perspective of privileged structures. Future Med. Chem. 9 (2017) 1765-1794.
18. S. Kasibhatla, V. Baichwal, S. X. Cai, B. Roth, I. Skvortsova, S. Skvortsov, P. Lukas, N. M. English, N. Sirisoma, J. Drewe, A. Pervin, B. Tseng, R. O. Carlson, C. M. Pleiman, MPC-6827: a small-molecule inhibitor of microtubule formation that is not a substrate for multidrug resistance pumps. Cancer Res. 67 (2007) 5865-5871.
19. N. Sirisoma, A. Pervin, H. Zhang, S. Jiang, J. A. Willardsen, M. B. Anderson, G. Mather, C. M. Pleiman, S. Kasibhatla, B. Tseng, J. Drewe, S. Cai, Discovery of N-(4-methoxyphenyl)-N,2-dimethylquinazolin-4-amine, a potent apoptosis inducer and efficacious anticancer agent with high blood brain barrier penetration. J. Med. Chem. 52 (2009) 2341-2351.
20. X. F. Wang, S. B. Wang, E. Ohkoshi, L. T. Wang, E. Hamel, K. Qian, S. L. Morris-Natschke, K. H. Lee, L. Xie, N-Aryl-6-methoxy-1,2,3,4-tetrahydroquinolines: A novel class of antitumor agents targeting the colchicine site on tubulin. Eur. J. Med. Chem. 67 (2013) 196-207.
21. X. Wang, F. Guan, E. Ohkoshi, W. Guo, L. Wang, D. Zhu, S. Wang, L. Wang, E. Hamel, D. Yang, L. Li, K. Qian, S. L. Morris-Natschke, S. Yuan, K. Lee, L. Xie, Optimization of 4-(N-cycloamino)phenylquinazolines as a novel class of tubulin-polymerization inhibitors targeting the colchicine site. J. Med. Chem. 57 (2014) 1390-1402.
22. S. Banerjee, K. E. Arnst, Y. Wang, G. Kumar, S. Deng, L. Yang, G. Li, J. Yang, S. W. White, W. Li, D. D. Miller, Heterocyclic-Fused pyrimidines as novel tubulin polymerization inhibitors targeting the colchicine binding site: structural basis and antitumor efficacy. J. Med. Chem. 61(2018) 1704-1718.
23. I. Khelifi, T. Naret, D. Renko, A. Hamze, G. Bernadat, J. Bignon, C. Lenoir, J. Dubois, J. Brion, O. Provot, M. Alami, Design, synthesis and anticancer properties of IsoCombretaQuinolines as potent tubulin assembly inhibitors. Eur. J. Med. Chem. 127 (2017)

1025-1034.

24. M. Soussi, O. Provot, G. Berbadat, J. Bignon, D. Desravines, J. Dubois, J. Brion, S. Messaoudi, M. Alami. IsoCombretaQuinazolines: potent cytotoxic agents with antitubulin activity. ChemMedChem 10 (2015) 1392-1402.
25. A. Brancale, R. Silvestr, Indole, a core nucleus for potent inhibitors of tubulin polymerization. Med. Res. Rev. 27 (2007) 209-238,
26. S. A. Patil, R. Patil, D. D. Miller, Indole molecules as inhibitors of tubulin polymerization: potential new anticancer agents. Future Med. Chem. 4 (2012) 2085-2115.
27. R. Patil, S. A. Patil, K. D. Beaman, S. A. Patil, Indole molecules as inhibitors of tubulin polymerization: potential new anticancer agents, an update (2013-2015). Future Med. Chem. 8 (2016) 1291-1316.
28. R. Álvarez, C. Gajate, P. Puebla, F. Mollinedo, M. Medarde, R. Peláez, Substitution at the indole 3 position yields highly potent indolecombretastatins against human tumor cells. Eur. J. Med. Chem. 158 (2018) 167-183.
29. R. Álvarez, P. Puebla, J. F. Díaz, A. C. Bento, R. G. Navas, J. Vicente, F. Mollinedo, J. M. Andreu, M. Medarde, R. Peláez, Endowing indole-based tubulin inhibitors with an anchor for derivatization: highly potent 3- substituted indolephenstatins and indoleisocombretastatins. J. Med. Chem. 56 (2013) 2813-2827.
30. J. Yan, J. Hu, B. An, L. Huang, X. Li, Design, synthesis, and biological evaluation of cyclic-indole derivatives as anti-tumor agents via the inhibition of tubulin polymerization. Eur. J. Med. Chem. 125 (2017) 663-675.
31. W. Li, Y. Yin, H. Yao, W. Shuai, H. Sun, S. Xu, J. Liu, H. Yao, Z. Zhu, J. Xu, Discovery of novel vinyl sulfone derivatives as anti-tumor agents with microtubule polymerization inhibitory and vascular disrupting activities. Eur. J. Med. Chem. 157 (2018) 1068-1080.
32. W. Li, W. Shuai, F. Xu, H. Sun, S. Xu, H. Yao, J. Liu, H. Yao, Z. Zhu, J. Xu, Discovery of novel 4-arylisochromenes as anticancer agents with inhibitory activity of tubulin polymerization. ACS Med. Chem. Lett. 9 (2018) 974-979.
33. W. Li, Y. Yin, W. Shuai, F. Xu, H. Yao; J. Liu, K. Cheng, J. Xu, Z. Zhu, S. Xu. Discovery of novel quinazolines as potential anti-tubulin agents occupying three zones of colchicine domain. Bioorg. Chem. 83 (2019) 380-390.
34. M. R. Buemi, L. D. Luca, S. Ferro, R. Gitto. Targeting GluN2B-containing *N*-methyl-*D*-aspartate receptors: design, synthesis, and binding affinity evaluation of novel 3-substituted indoles. Arch. Pharm. Chem. Life Sci. 347 (2014) 533-539.
35. T. He, X. Tao, X. Wu, L. Cai, V. W. P, Acetylation of N-heteroaryl bromides via $PdCl_2$/(o-tolyl)$_3$P catalyzed Heck reactions. Synthesis, 6 (2008) 887-890.
36. B. M. Trost, A. McClory, Rhodium-catalyzed cycloisomerization: formation of indoles, benzofurans, and enol lactones. Angew. Chem. Int. Ed. 46 (2007) 2074-2077.